The Astronomical Journal, 149:91 (28pp), 2015 March doi:10.1088/0004-6256/149/3/91

THE *HUBBLE SPACE TELESCOPE* UV LEGACY SURVEY OF GALACTIC GLOBULAR CLUSTERS. I. OVERVIEW OF THE PROJECT AND DETECTION OF MULTIPLE STELLAR POPULATIONS*

G. Piotto[1,2], A. P. Milone[3], L. R. Bedin[2], J. Anderson[4], I. R. King[5], A. F. Marino[3], D. Nardiello[1,2], A. Aparicio[6,7], B. Barbuy[8], A. Bellini[4], T. M. Brown[3], S. Cassisi[9], A. M. Cool[10], A. Cunial[1,2], E. Dalessandro[11], F. D'Antona[12], F. R. Ferraro[11], S. Hidalgo[6,7], B. Lanzoni[11], M. Monelli[6,7], S. Ortolani[1,2], A. Renzini[2], M. Salaris[13], A. Sarajedini[14], R. P. van der Marel[4], E. Vesperini[15], and M. Zoccali[16,17]

[1] Dipartimento di Fisica e Astronomia "Galileo Galilei," Università di Padova, Vicolo dell'Osservatorio 3, I-35122 Padova, Italy; giampaolo.piotto@unipd.it, domenico.nardiello@studenti.unipd.it, andrea.cunial@studenti.unipd.it, sergio.ortolani@unipd.it
[2] INAF-Osservatorio Astronomico di Padova, Vicolo dell'Osservatorio 5, I-35122 Padova, Italy; luigi.bedin@oapd.inaf.it, alvio.renzini@oapd.inaf.it
[3] Research School of Astronomy and Astrophysics, The Australian National University, Cotter Road, Weston, ACT, 2611, Australia; milone@mso.anu.edu.au, amarino@mso.anu.edu.au
[4] Space Telescope Science Institute, 3700 San Martin Drive, Baltimore, MD 21218, USA; jayander@stsci.edu, bellini@stsci.edu, tbrown@stsci.edu, marel@stsci.edu
[5] Department of Astronomy, University of Washington, Box 351580, Seattle, WA 98195-1580; king@astro.washington.edu
[6] Instituto de Astrofísica de Canarias, E-38200 La Laguna, Tenerife, Canary Islands, Spain; antapaj@iac.es, shidalgo@iac.es, monelli@iac.es
[7] Department of Astrophysics, University of La Laguna, E-38200 La Laguna, Tenerife, Canary Islands, Spain
[8] Universidade de Sao Paulo, IAG, Rua do Matao 1226, Cidade Universitaria, Sao Paulo 05508-900, Brazil; barbuy@astro.iag.usp.br
[9] Osservatorio Astronomico di Teramo, Via Mentore Maggini s.n.c., I-64100 Teramo, Italy; cassisi@oateramo.inaf.it
[10] Department of Physics and Astronomy, San Francisco State University, 1600 Holloway Avenue, San Francisco, CA 94132, USA; cool@sfsu.edu
[11] Dipartimento di Fisica e Astronomia, Università degli Studi di Bologna, Viale Berti Pichat 6/2, I-40127 Bologna, Italy; emanuele.dalessandr2@unibo.it, francesco.ferraro3@unibo.it, barbara.lanzoni3@unibo.it
[12] INAF-Osservatorio Astronomico di Roma, Via Frascati 33, I-00040 Monteporzio Catone, Roma, Italy; dantona@oa-roma.inaf.it
[13] Astrophysics Research Institute, Liverpool John Moores University, Liverpool Science Park, IC2 Building, 146 Brownlow Hill, Liverpool L3 5RF, UK; ms@astro.livjm.ac.uk
[14] Department of Astronomy, University of Florida, 211 Bryant Space Science Center, Gainesville, FL 32611, USA; ata@astro.ufl.edu
[15] Department of Astronomy, Indiana University, Bloomington, IN 47405, USA; evesperi@indiana.edu
[16] Instituto de Astrofísica, Pontificia Universidad Católica de Chile, Av. Vicuña Mackenna 4860, Macul, Santiago de Chile; mzoccali@astro.puc.cl
[17] Millennium Institute of Astrophysics, Av. Vicuña Mackenna 4860, Macul, Santiago de Chile
Received 2014 August 20; accepted 2014 October 9; published 2015 February 5

ABSTRACT

In this paper we describe a new UV-initiative *Hubble Space Telescope* project (GO-13297) that will complement the existing F606W and F814W database of the Advanced Camera for Surveys Globular Cluster (GC) Treasury by imaging most of its clusters through UV/blue WFC3/UVIS filters F275W, F336W, and F438W. This "magic trio" of filters has shown an uncanny ability to disentangle and characterize multiple population (MP) patterns in GCs in a way that is exquisitely sensitive to C, N, and O abundance variations. Combination of these passbands with those in the optical also gives the best leverage for measuring helium enrichment. The dozen clusters that had previously been observed in these bands exhibit a bewildering variety of MP patterns, and the new survey will map the full variance of the phenomenon. The ubiquity of multiple stellar generations in GCs has made the formation of these cornerstone objects more intriguing than ever; GC formation and the origin of their MPs have now become one and the same problem. In this paper we will describe the database and our data reduction strategy, as well as the uses we intend to make of the final photometry, astrometry, and PMs. We will also present preliminary color–magnitude diagrams from the data so far collected. These diagrams also draw on data from GO-12605 and GO-12311, which served as a pilot project for the present GO-13297.

Key words: globular clusters: general – Hertzsprung–Russell and C–M diagrams – proper motions – stars: Population II

1. INTRODUCTION

It was once thought that we understood how globular clusters (GCs) formed in the early universe, but recent discoveries of their multiple populations (MPs) have unraveled our long-held view of GCs as "simple stellar populations" formed in a single burst. It now appears that virtually *all* of them host multiple stellar generations, with secondary populations characterized by puzzling chemical compositions. After almost a decade since the first breakthrough (Bedin et al. 2004), our current understanding can be summarized as follows.

1. *Ubiquity*. Almost all GCs that have been adequately studied are composed of distinct stellar populations (Piotto et al. 2012), from two in number up to six or more (Omega Centauri (ω Cen), Bellini et al. 2010). Even clusters not yet sufficiently probed photometrically exhibit the telling Na–O anti-correlation in the spectra of their giant stars (Carretta et al. 2009). An exception is Rup 106. Villanova et al. (2013) have analyzed spectra of nine red giant branch (RGB) stars, and concluded that this GC hosts a single stellar population. In addition, Walker et al. (2011) claimed that IC 4499 does not show evidence of MPs. In both cases, higher precision stellar photometry is needed for a definitive conclusion on the nature of the stellar populations in these two GCs.

* Based on observations with the NASA/ESA *Hubble Space Telescope*, obtained at the Space Telescope Science Institute, which is operated by AURA, Inc., under NASA contract NAS 5-26555.

Table 1

List of the Clusters and Corresponding Observations (Mainly from GO-13297) Presented in this Paper. The Final Five Columns Give the Galactic *XYZ* Coordinates, the Reddening, and the Distance Modulus

		Primary Fields			Parallel Fields		GO-10775 Fields						
Cluster	# Orbits	Exp. Time F275W(s)	Exp. Time F336W(s)	Exp. Time F438W(s)	Exp. Time F475W(s)	Exp. Time F814W(s)	Exp. Time F606W(s)	Exp. Time F814W(s)	X (kpc)	Y (kpc)	Z (kpc)	$E(B-V)$	$(m-M)_V$
NGC 104[a]	2	12 × 348, 2 × 323	⋯	⋯	2 × 265	⋯	4 × 50, 3	4 × 50, 3	−6.4	−2.6	−2.7	0.04	13.37
NGC 288[b]	2	6 × 401	4 × 350	4 × 41	⋯	⋯	3 × 10, 12 × 130	3 × 10, 12 × 150	−8.4	0.0	−8.5	0.03	14.84
NGC 362[b]	2	6 × 519	4 × 350	4 × 54	⋯	⋯	4 × 150, 10	4 × 170, 10	−5.2	−5.1	−5.8	0.05	14.83
NGC 1261	5	4 × 834, 2 × 855, 2 × 859, 2 × 918	2 × 413, 2 × 415, 419	164, 165, 167, 168, 170	2 × 745, 766, 770, 829	2 × 669, 690, 697, 753	5 × 350, 40	5 × 360, 40	−8.2	−10.0	−12.5	0.01	16.09
NGC 1851	1	⋯	4 × 453	2 × 140	⋯	⋯	5 × 350, 20	5 × 350, 20	−12.5	−8.9	−6.5	0.02	15.47
NGC 1851[a]	7	14 × 1280	⋯	⋯	7 × 40 7 × 947	7 × 976	⋯	⋯	⋯	⋯	⋯	⋯	⋯
NGC 2808[b]	6	12 × 985	6 × 650	6 × 97	6 × 890, 6 × 982	6 × 508	5 × 360, 23	5 × 370, 23	−6.3	−9.2	−1.5	0.22	15.59
NGC 2298	4	4 × 848, 2 × 980, 2 × 981	4 × 350	2 × 134, 136,137	2 × 785, 885, 887	2 × 683, 815, 816	5 × 350, 20	5 × 350, 20	−12.6	−9.4	−2.6	0.14	15.60
NGC 3201	2	2 × 754, 2 × 758	4 × 310	60, 68	685, 689	612, 616	1 × 5, 4 × 100,	1 × 5, 4 × 100	−7.7	−4.8	1.1	0.24	14.20
NGC 4590 (M68)	2	4 × 696	4 × 305	2 × 60	2 × 627	2 × 554	4 × 130, 12	4 × 150, 12	−4.2	−7.2	6.4	0.05	15.21
NGC 4833	4	4 × 936, 4 × 895	4 × 350	2 × 136, 135,138	2 × 806, 2 × 840	2 × 771, 2 × 730	1 × 10, 4 × 150,	1 × 10, 4 × 170,	−4.7	−5.4	−0.5	0.32	15.08
NGC 5024 (M53)	6	2 × 1733, 2 × 1832, 1729	3 × 433, 3 × 460	3 × 170, 2 × 180, 178	2 × 1451, 2 × 1550, 1447, 1548	3 × 370, 3 × 375	5 × 340, 45	5 × 340, 45	−5.5	−1.4	18.0	0.02	16.32
NGC 5053	5	4 × 829, 4 × 879, 2 × 854	5 × 415	2 × 164, 3 × 65,	2 × 740, 2 × 790, 765	2 × 664, 2 × 714, 689	5 × 340, 30	5 × 350, 30	−5.3	−1.4	17.5	0.01	16.23
NGC 5272 (M3)[b]	2	6 × 415	4 × 350	4 × 42	⋯	⋯	4 × 130, 12	4 × 150, 12	−6.8	1.3	10.4	0.01	15.07
NGC 5286	2	2 × 797, 2 × 668	4 × 310	65, 66	728, 603	655, 559	5 × 350, 30	5 × 360, 30	−0.7	−8.6	2.5	0.24	16.08

Table 1
(Continued)

Cluster	# Orbits	Primary Fields			Parallel Fields		GO-10775 Fields		X (kpc)	Y (kpc)	Z (kpc)	$E(B-V)$	$(m-M)_V$
		Exp. Time F275W(s)	Exp. Time F336W(s)	Exp. Time F438W(s)	Exp. Time F475W(s)	Exp. Time F814W(s)	Exp. Time F606W(s)	Exp. Time F814W(s)					
NGC 5466	4	2 × 930, 2 × 928, 4 × 865	4 × 350	2 × 135, 138, 139	2 × 776, 834, 835	2 × 700, 763, 765	5 × 340, 30	5 × 350, 30	−5.0	3.0	15.7	0.00	16.02
NGC 5897	4	4 × 926, 2 × 875, 2 × 874	4 × 350	3 × 140, 138	779, 781, 830, 833	2 × 761, 710, 709	5 × 340, 25	5 × 350, 25	2.0	−3.2	6.7	0.09	15.76
NGC 5904 (M5)	2	2 × 689, 2 × 690	4 × 306	58, 59	620, 621	2 × 559	4 × 140, 7	4 × 140, 7	−3.2	0.3	5.9	0.03	14.46
NGC 5927	2	4 × 668	4 × 310	2 × 66	2 × 603	2 × 559	5 × 350, 30	5 × 350, 25	−1.9	−4.2	1.1	0.45	15.82
NGC 5986	2	2 × 745, 2 × 668	4 × 300	60, 64	676, 603	603, 559	5 × 350, 20	5 × 350, 20	1.0	−4.0	2.8	0.28	15.96
NGC 6093 (M80)[b]	5	10 × 885	6 × 657	6 × 85	5 × 760, 5 × 845	5 × 539	5 × 340, 10	5 × 340, 10	1.1	−1.2	3.7	0.18	15.56
NGC 6101	5	4 × 851, 4 × 889, 2 × 940	5 × 415	4 × 165, 167	2 × 762, 2 × 800, 851	2 × 686, 2 × 724, 775	5 × 370, 35	5 × 380, 35	2.7	−10.0	−3.8	0.05	16.10
NGC 6121 (M4)	2	2 × 808, 2 × 735	4 × 300	66, 65	666, 739	593, 666	1 × 1.5, 2 × 25, 2 × 30	1 × 1.5, 4 × 30	−6.2	−0.3	1.0	0.35	12.82
NGC 6121 (M4)[a]	2	10 × 380											
NGC 6144	2	4 × 748	4 × 304	2 × 61	2 × 679	2 × 606	5 × 340, 25	5 × 350, 25	0.2	−1.2	2.8	0.36	15.86
NGC 6171	4	4 × 926, 2 × 896, 2 × 895	4 × 350	2 × 136, 138, 140	800, 802, 830, 833	2 × 761, 730, 731	4 × 130, 12	4 × 150, 12	−2.4	0.3	2.9	0.33	15.05
NGC 6205 (M13)[b]	2	6 × 427	4 × 350	4 × 46	⋯	⋯	4 × 140, 7	4 × 140, 7	−5.5	4.6	5.1	0.02	14.33
NGC 6218 (M12)	2	2 × 790, 2 × 714	4 × 306	58, 66	645, 721	572, 648	4 × 90, 4	4 × 90, 4	−4.1	1.2	2.5	0.19	14.01
NGC 6254 (M10)	2	2 × 790, 2 × 713	4 × 306	60, 66	644, 721	571, 648	4 × 90, 4	4 × 90, 4	−4.4	1.1	2.1	0.28	14.08
NGC 6304	2	2 × 693,	4 × 304	60, 61	624, 731	559, 658	5 × 340,	5 × 350,	−2.5	−0.4	1.0	0.54	15.52

Table 1
(Continued)

Cluster	# Orbits	Primary Fields			Parallel Fields		GO-10775 Fields		X (kpc)	Y (kpc)	Z (kpc)	$E(B-V)$	$(m-M)_V$
		Exp. Time F275W(s)	Exp. Time F336W(s)	Exp. Time F438W(s)	Exp. Time F475W(s)	Exp. Time F814W(s)	Exp. Time F606W(s)	Exp. Time F814W(s)					
		2 × 800					20	20					
NGC 6341 (M92)	2	2 × 707, 2 × 819	4 × 304	57, 59	638, 750	565, 677	4 × 140, 7	4 × 150, 7	−5.8	6.3	5.1	0.02	14.65
NGC 6352	2	2 × 706, 2 × 800	4 × 311	58, 72	637, 731	564, 658	4 × 140, 7	4 × 150, 7	−3.0	−1.8	−0.3	0.22	14.43
NGC 6362	2	2 × 720, 2 × 829	4 × 323	68, 67	651, 760	578, 687	4 × 130, 10	4 × 150, 10	−2.3	−4.1	−1.9	0.09	14.68
NGC 6366	2	2 × 795, 2 × 713	4 × 305	2 × 62	644, 726	571, 653	4 × 140, 10	4 × 140, 10	−5.1	1.1	1.4	0.71	14.94
NGC 6388	4	2 × 889, 2 × 888, 2 × 999, 2 × 961	4 × 350	2 × 135, 2 × 133	793, 795, 865, 906	723, 724, 796, 834	5 × 340, 40	5 × 350, 40	1.3	−2.5	−0.8	0.37	16.13
NGC 6397	2	2 × 709, 2 × 752	4 × 310	2 × 66	640, 683	567, 610	4 × 15, 1	4 × 15, 1	−6.2	−0.8	−0.1	0.18	12.37
NGC 6441	4	2 × 887, 2 × 890, 2 × 928, 2 × 929	4 × 350	123, 126, 128, 129	2 × 794, 833, 835	722, 725, 763, 764	5 × 340, 45	5 × 350, 45	3.2	−1.3	−0.6	0.47	16.78
NGC 6496	2	2 × 707, 2 × 800	4 × 303	61, 73	638, 731	565, 658	10 × 340, 2 × 30	5 × 350, 30	2.6	−2.3	−1.6	0.15	15.74
NGC 6535	2	2 × 713, 2 × 793	4 × 305	2 × 62	644, 724	571, 651	4 × 130, 12	4 × 150, 12	−2.3	3.1	1.6	0.34	15.22
NGC 6541	2	2 × 708, 2 × 758	4 × 300	65, 66	639, 689	566, 616	4 × 140, 8	4 × 150, 8	−1.0	−1.4	−1.1	0.14	14.82
NGC 6584	2	2 × 709, 2 × 795	4 × 312	62, 65	640, 726	567, 653	5 × 350, 25	5 × 360, 25	4.0	−4.0	−3.4	0.1	15.96
NGC 6624	2	2 × 707, 2 × 800	4 × 295	62, 81	638, 731	565, 658	5 × 350, 15	5 × 350, 15	−0.5	0.4	−0.7	0.28	15.36
NGC 6637 (M69)	4	2 × 887, 2 × 888, 2 × 923, 2 × 933	4 × 350	120, 122, 130, 131	792, 794 827, 840	722, 723, 758, 768	5 × 340, 18	5 × 340, 18	0.3	0.3	−1.2	0.18	15.28

Table 1
(Continued)

Cluster	# Orbits	Primary Fields			Parallel Fields		GO-10775 Fields		X (kpc)	Y (kpc)	Z (kpc)	$E(B-V)$	$(m-M)_V$
		Exp. Time F275W(s)	Exp. Time F336W(s)	Exp. Time F438W(s)	Exp. Time F475W(s)	Exp. Time F814W(s)	Exp. Time F606W(s)	Exp. Time F814W(s)					
NGC 6652	3	2 × 690, 2 × 775, 2 × 800	2 × 305, 3 × 313, 312	60, 69, 86	621, 707, 733	548, 633, 658	5 × 340, 18	5 × 340, 18	1.5	0.3	−1.6	0.09	15.28
NGC 6656 (M22)	1	…	3 × 475, 476	2 × 141	…	…	4 × 55, 3	5 × 65, 3	−5.1	0.6	−0.0	0.34	13.60
NGC 6656 (M22)[a]	4	12 × 800	…	…	4 × 644	4 × 339	…	…	…	…	…	…	…
NGC 6681 (M70)	2	2 × 706, 2 × 800	4 × 294	66, 83	637, 730	564, 658	4 × 140, 10	4 × 150, 10	0.5	0.4	−1.6	0.07	14.99
NGC 6715 (M54)	6	3 × 1755, 2 × 1920, 1916	3 × 433, 3 × 475	3 × 170, 3 × 190	3 × 370, 3 × 390	2 × 1638, 1469, 1473, 1474, 1634	4 × 340, 30	4 × 350, 30	17.3	2.5	−6.1	0.15	17.58
NGC 6717	3	4 × 686, 2 × 687	5 × 313, 311	3 × 60	2 × 619, 617	2 × 544, 535	4 × 130, 10	4 × 150, 10	−1.5	1.6	−0.9	0.22	14.94
NGC 6723	3	4 × 693, 2 × 734	6 × 313	2 × 61, 60	624, 626, 666	2 × 551, 592	4 × 140, 10	4 × 150, 10	−0.0	0.0	−2.2	0.05	14.84
NGC 6752[a]	2	12 × 360	…	…	2 × 265	…	4 × 35, 2	4 × 40, 2	−5.0	−1.4	−1.3	0.04	13.13
NGC 6779 (M56)	2	2 × 706, 2 × 800	4 × 295	64, 81	637, 731	564, 658	5 × 340, 20	5 × 350, 20	−4.0	8.3	1.8	0.26	15.68
NGC 6791	2	2 × 700, 2 × 707	2 × 297, 2 × 300	65, 72	631, 638	559, 565	…	…	−3.5	−1.7	1.4	0.12	13.43
NGC 6809 (M55)	2	2 × 746, 2 × 822	4 × 294	64, 66	677, 753	604, 680	4 × 70, 4	4 × 80, 4	−3.4	0.8	−1.7	0.08	13.89
NGC 6838 (M71)	2	2 × 750, 2 × 792	4 × 303	2 × 65	681, 723	608, 650	4 × 75, 4	4 × 80, 4	−6.1	3.4	0.1	0.25	13.80
NGC 6934	2	2 × 713, 2 × 792	4 × 304	64, 70	644, 723	571, 650	5 × 340, 45	5 × 340, 45	0.8	11.7	−4.7	0.1	16.28
NGC 6981 (M72)	2	2 × 693, 2 × 710	2 × 304, 2 × 305	64, 70	624, 641	551, 568	4 × 130, 10	4 × 150, 10	3.4	8.3	−8.8	0.05	16.31
NGC 7078 (M15)[b]	3	3 × 615, 3 × 700	6 × 350	6 × 65	…	…	4 × 130, 15	4 × 150, 15	−4.4	8.3	−4.4	0.1	15.39

Table 1
(Continued)

Cluster	# Orbits	Primary Fields			Parallel Fields		GO-10775 Fields		X (kpc)	Y (kpc)	Z (kpc)	$E(B-V)$	$(m-M)_V$
		Exp. Time F275W(s)	Exp. Time F336W(s)	Exp. Time F438W(s)	Exp. Time F475W(s)	Exp. Time F814W(s)	Exp. Time F606W(s)	Exp. Time F814W(s)					
NGC 7089 (M2)	3	2 × 676, 2 × 735, 2 × 785	6 × 313	2 × 62, 70	611, 668, 717	534, 593, 643	5 × 340, 20	5 × 340, 20	−2.7	7.5	−6.3	0.06	15.50
NGC 7099 (M30)	2	4 × 725	4 × 303	2 × 65	2 × 656	2 × 583	4 × 140, 7	4 × 140, 7	−3.4	2.5	−5.5	0.03	14.64

[a] Data from GO-12311.
[b] Data from GO-12605.

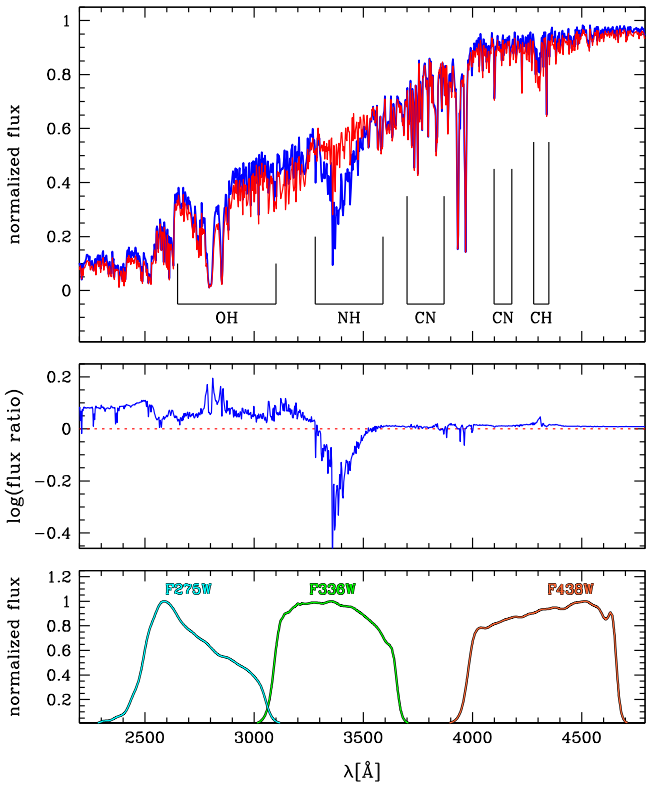

Figure 1. Upper panel: in red the simulated spectrum of a star of the first stellar generation (N-poor) RGBa in NGC 6752; in blue the simulated spectrum of a third generation, N-rich, RGBc star (Milone et al. 2010). Middle panel: flux ratio of the two spectra reproduced in the upper panel. Lower panel: bandpasses of WFC3/UVIS with F275W, F336W, and F438W.

2. *Enrichment*. While the first-generation (1G) stars have a composition that can be ascribed to the proto-galactic interstellar matter out of which they formed, the second-generation (2G) stars can be depleted in C and O, enhanced in N and Na (e.g., Carretta et al. 2009; Marino et al. 2008, 2011a, 2011b, 2012, 2014), and enhanced in He (Milone et al. 2012a, 2012b, 2014a). In some cases the He enhancement can be quite strong, close to $Y = 0.40$ (e.g., D'Antona & Caloi 2004; Norris 2004; Piotto et al. 2005, 2007; King et al. 2012; Bellini et al. 2013a), while in others it is still measurable but small (e.g., ∼0.01 as in the cases of NGC 6397, Milone et al. 2012b, and NGC 288, Piotto et al. 2013). This chemical pattern indicates that the material out of which GCs formed was exposed to proton-capture processes at high temperatures and must have come from relatively massive 1G stars. With a few notable exceptions, i.e., ω Cen (Norris & Da Costa 1995), M22 (Marino et al. 2009, 2011c), M54 (Carretta et al. 2010), NGC 1851 (Yong & Grundahl 2008), M2 (Yong et al. 2014), NGC5 824 (Da Costa et al. 2014), and Terzan 5 (Ferraro et al. 2009a), 2G stars have the same abundances of iron and other heavy-elements as the 1G stars, indicating that their material was somehow not tainted by 1G supernova products. Even in the case of clusters exhibiting multiple iron abundances, the differences are relatively small, indicating that only a tiny fraction of the supernova products from 1G were incorporated in 2G stars (Renzini 2013). It is not clear at present whether the clusters with iron abundance variations are part of a different class of GCs. Because of the large number of GCs sampled, GO-13297 will surely help to address this idea.
3. *Variety*. Thus far, we have found no two clusters that manifest the MP phenomenon in the same way. The relative proportion of 1G to 2G stars differs enormously from one GC to another, and in several cases the 2G stars outnumber 1G stars and are more centrally concentrated (as in ω Cen; Bellini et al. 2010, and 47 Tuc, Milone et al. 2012a, see also Lardo et al. 2011, but based on lower quality SDSS data.), becoming quite dominant at the very center. In other cases, large differences are also seen in the degree of He enhancement and in p-capture elements.
4. *Discreteness*. One crucial property of MPs is that in a large number of GCs the populations can be separated into quite distinct sequences within each color–magnitude diagram (CMD) and/or in appropriate two-color plots, as opposed to a continuous spread, observational results that any formation scenario must be able to account for.

Different progenitors of the 2G have been proposed. Intermediate-mass asymptotic giant branch (AGB-M) stars (D'Antona et al. 2002), fast-rotating massive stars (FRMS) (Decressin et al. 2007), or interacting massive binary stars (de Mink et al. 2009; Vanbeveren et al. 2012) may eject materials with composition similar to that of 2G stars, i.e., somewhat helium enriched and exposed to proton capture reactions at high temperatures, but with sizable differences from one case to another.

The AGB-M and the FRMS models are those for which all the different aspects of the study of MPs have been more extensively investigated. Although these models are based on different sources of processed gas, in both models the amount of gas available for 2G formation is only a small fraction of the initial 1G. This has the important implication that both these models require the 1G star cluster to be initially more massive than it is now (see e.g., Decressin et al. 2007; D'Ercole et al. 2008; Renzini 2008, 2013; Ventura et al. 2014 for estimates of the possible initial 1G cluster masses), and to have undergone a significant loss of 1G stars (see, e.g., D'Ercole et al. 2008; Decressin et al. 2010), leading to the large fraction of 2G stars currently observed in many GCs (Renzini 2008). This large loss of 1G stars also implies that GCs must have significantly contributed to the formation of the Galactic halo (see e.g., Vesperini et al. 2010; Schaerer & Charbonnel 2011). Another requirement shared by these models is that not only ejected material from the 1G stars is necessary. It may have been somehow diluted with gas with the same composition as the 1G in order to reproduce the Na–O anticorrelation (as advocated by Decressin et al. 2007; D'Ercole et al. 2008, 2011), though the mode of such dilution remain obscure. The origin of this pristine gas is still a matter of investigation and debate. Curiously, recent surveys of young (10 Myr–1 Gyr) extra-galactic massive clusters (Bastian et al. 2013a) do not show any evidence of the presence of gas and/or ongoing star formation, though the facts are not quite clear on this (Vinkó et al. 2009). Recently Bastian et al. (2013b), following an earlier suggestion by D'Antona et al. (1983), proposed a model which would not require a larger 1G cluster mass and is based on the accretion of enriched material released from interacting massive binaries and rapidly rotating stars onto their circum-stellar disks, and ultimately onto the young pre-main sequence stars. This model requires some very ad hoc assumptions (see D'Antona et al. 2014; Salaris & Cassisi 2014) both regarding

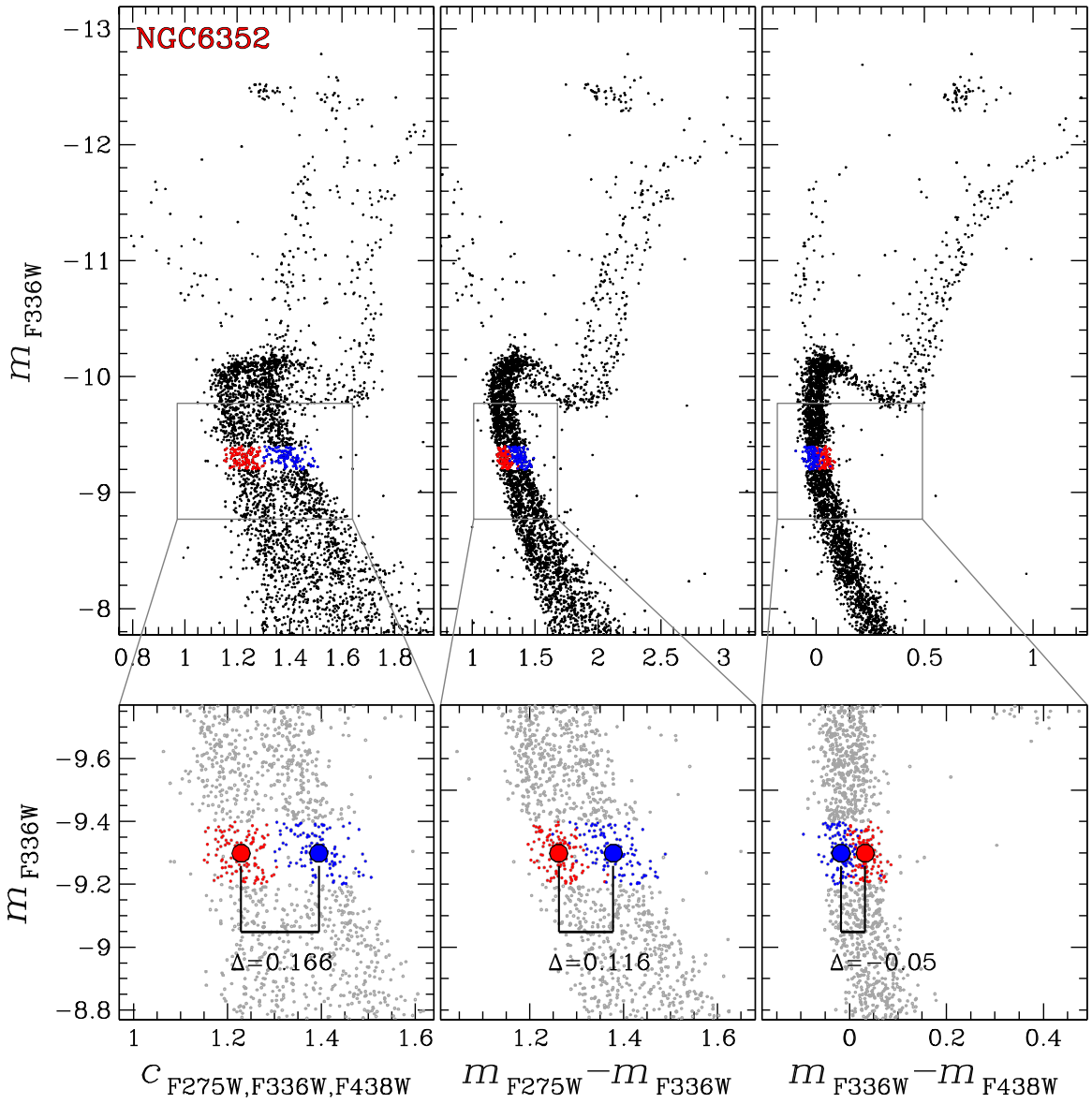

Figure 2. CMDs of NGC 6352 from GO-13297 data. m_{F336W} vs. $C_{F275W,F336W,F438W}$ (left panels), m_{F336W} vs. $m_{F275W} - m_{F336W}$ (middle panels), and m_{F336W} vs. $m_{F336W} - m_{F438W}$ (right panels). Lower panels show a zoom of the MS. Red dots highlight 2G stars; blue dots 1G stars.

the lifetimes of the pre-main sequence accretion disk and regarding the He content of the accreting material. Most importantly, the accretion scenario has serious difficulties in accounting for the discreteness of the sequences we observe in the CMDs.

In summary, the series of events that led from massive gas clouds in the early universe to the GCs we see today remains an intriguing puzzle. Clearly, GC formation was a far more complex process than ever imagined before. Clues and insight needed to solve this puzzle can come only from homogeneous mapping of a large sample of GCs with appropriate multi-band photometry. A photometric survey can map a large sample of stars at all evolutionary phases. Such a survey will enable us to identify 2G stars even in the cases where they represent a minor fraction of the entire cluster population. Multi-band photometry allows us to infer chemical properties of stars in a complementary way to spectroscopy (Milone et al. 2012a), and to do this for a large sample of GCs. This is the subject of the GO-13297 *Hubble Space Telescope* (*HST*) Large Treasury project (PI G. Piotto) approved for Cycle 21. This paper will describe in detail the project, the selected sample of clusters (see Table 1), the observational strategy, the data-reduction strategy, and the intended use of the data by the team. We will also present preliminary results from the data acquired thus far.

2. THE MAGIC OF WFC3'S UV FILTERS

Previous studies based on spectroscopy and ground-based photometry have shown that Strömgren and ultraviolet photometry does a good job in separating MPs along the RGB on nearby GCs (e.g., Marino et al. 2008; Yong et al. 2008). Our WFC3/UVIS observations in Cycles 18–20 have opened a spectacular new window by showing that UV/optical colors separate the various sub-populations much better than the traditional optical colors alone (Bellini et al. 2010, 2013a; Milone et al. 2010, 2012a, 2012b; Piotto et al. 2012, 2013) and do so across the *entire* CMD, from the main sequence (MS) all the way to the horizontal branch (HB). Figure 1 shows the

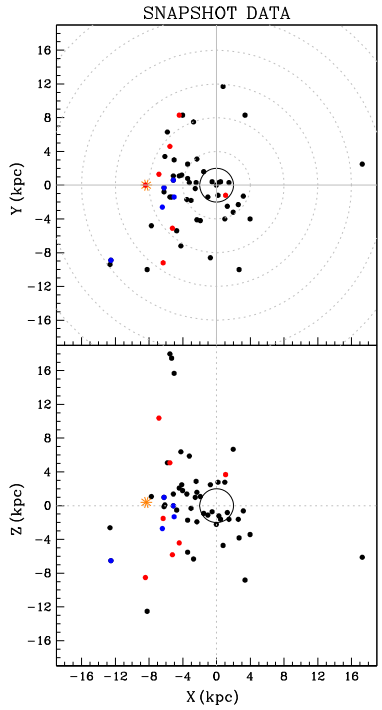

Figure 3. Spatial distribution of the target clusters for GO-13297 (black), GO-12605 (red), and GO-12311 (blue), in Galactic *XYZ* coordinates. The adopted Sun position is indicated by an asterisk.

power of the UV photometry for the case of NGC 6752. It reproduces the simulated spectra of RGBa (N-poor, He-poor red line, first stellar generation) and RGBc (N-rich, He-rich blue line, third stellar generation) of NGC 6752 (Milone et al. 2010).

The reason why F275W, F336W, and F438W work so well is quite simple. Milone et al. (2012a) emphasized that the F275W passband includes an OH molecular band, F336W an NH band, and F438W (or F435W for Advanced Camera for Surveys (ACS)) CN and CH bands, as illustrated in Figure 1. This property of the *HST* filter system is at the basis of the project we are presenting in this paper. The 1G stars, which are oxygen- and carbon-rich and nitrogen-poor, are relatively faint in F275W and F438W, but bright in F336W. Conversely, 2G stars, whose material has been CNO-cycle processed, are oxygen- and carbon-poor but nitrogen-rich. As a consequence, they are relatively bright in F275W and F438W but faint in F336W. Therefore, 1G stars are bluer than 2G stars in one color (F336W – F438W), but redder in another (F275W – F336W), and this *inversion* is seen in Figure 1. Milone et al. (2013) defined a pseudo-color $C_{\rm F275W,F336W,F438W} = (m_{\rm F275W} - m_{\rm F336W}) - (m_{\rm F336W} - m_{\rm F438W})$, which maximizes the virtue of both F336W – F438W and F275W – F336W, and has proven to be quite efficient in the separation of multiple sequences.

Figure 2 shows an example of the application of GO-13297 data to NGC 6352. The left panels show the power of the pseudo-color $C_{\rm F275W,F336W,F438W}$ in separating the two MSs. The middle panels show that in the $m_{\rm F336W}$ versus

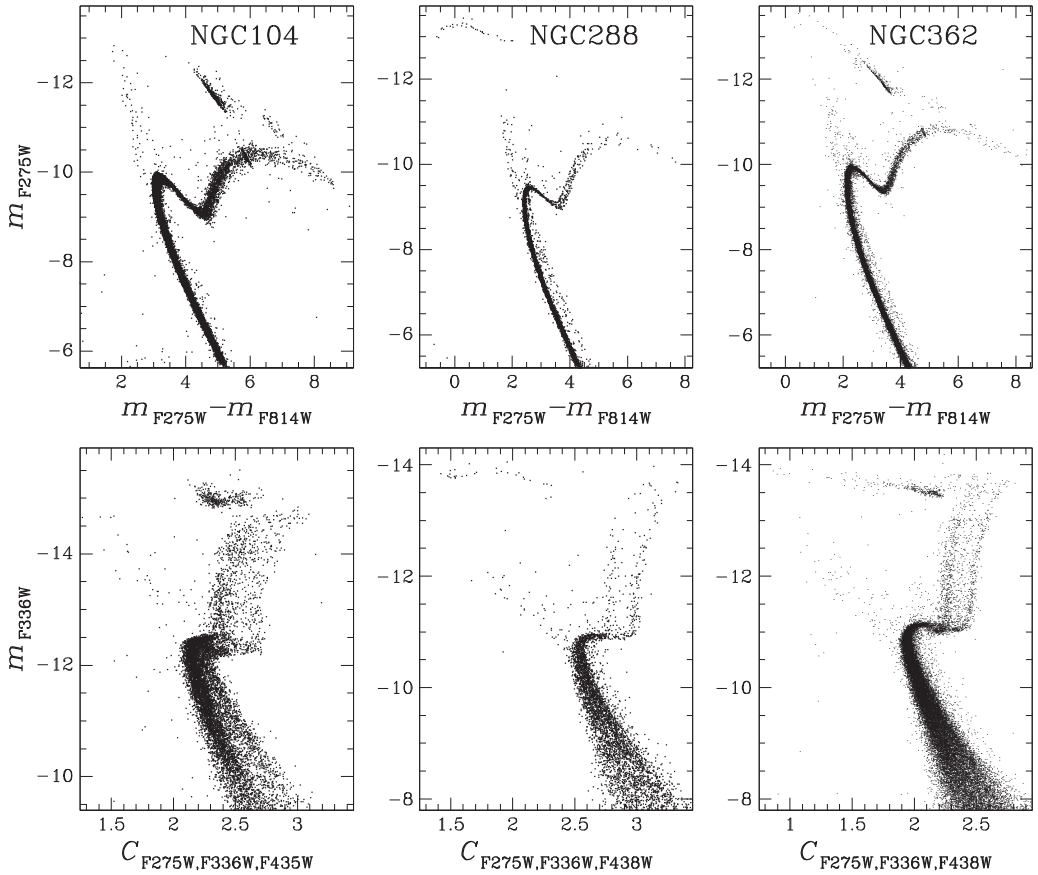

Figure 4. Upper panel: $m_{\rm F275W}$ vs. $m_{\rm F275W} - m_{\rm F814W}$ CMDs of NGC 104, NGC 288, and NGC 362. Lower panel: $m_{\rm F336W}$ vs. $C_{\rm F275W,F336W,F438W}$ index for the same clusters as the upper panel. Magnitudes and colors are in the instrumental system described in the text.

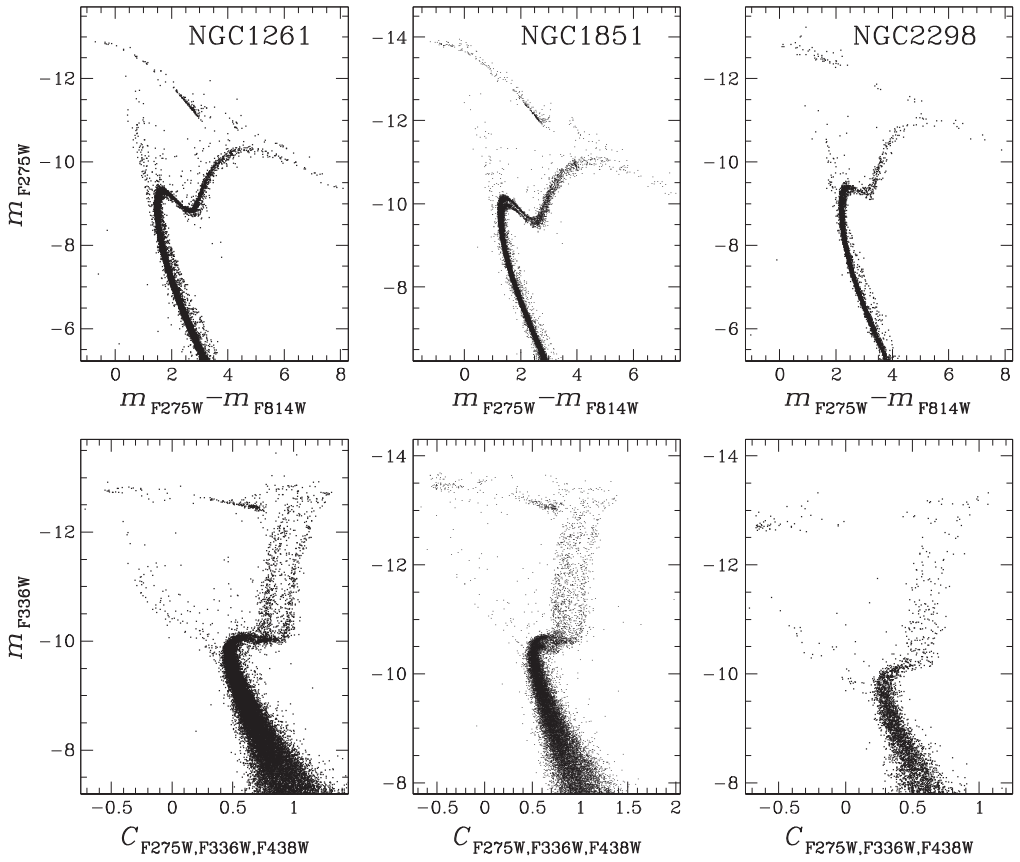

Figure 5. As in Figure 4 for NGC 1261, NGC 1851, and NGC 2298.

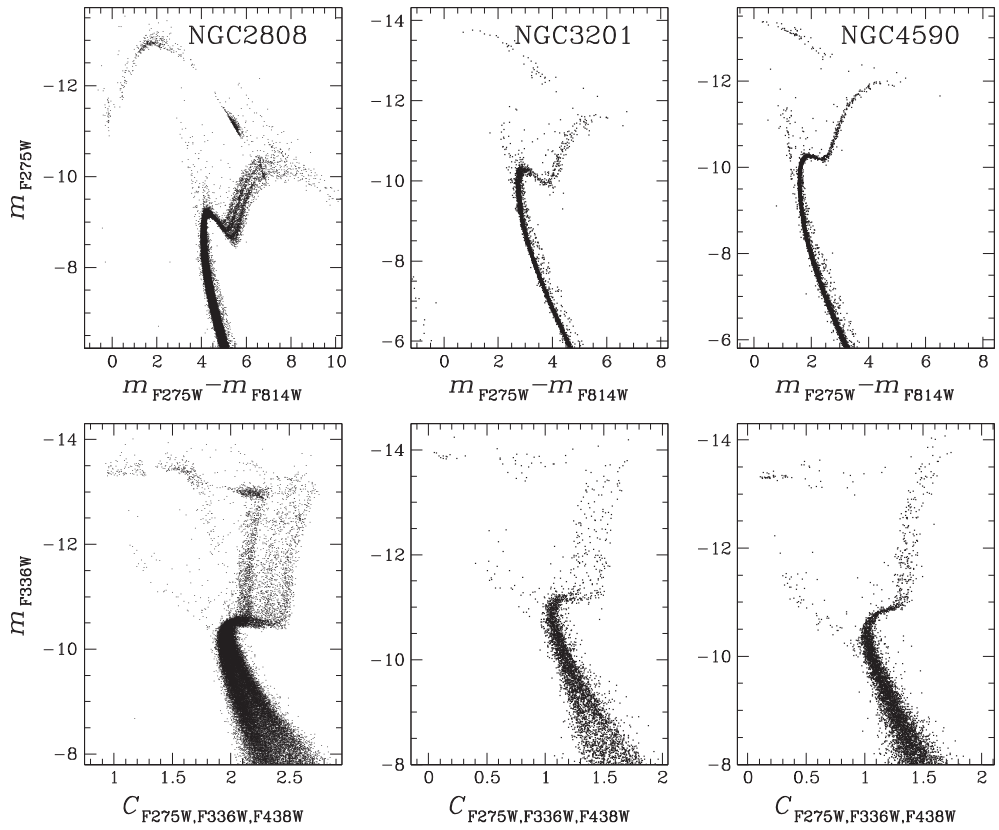

Figure 6. As in Figure 4 for NGC 2808, NGC 3201, and NGC 4590.

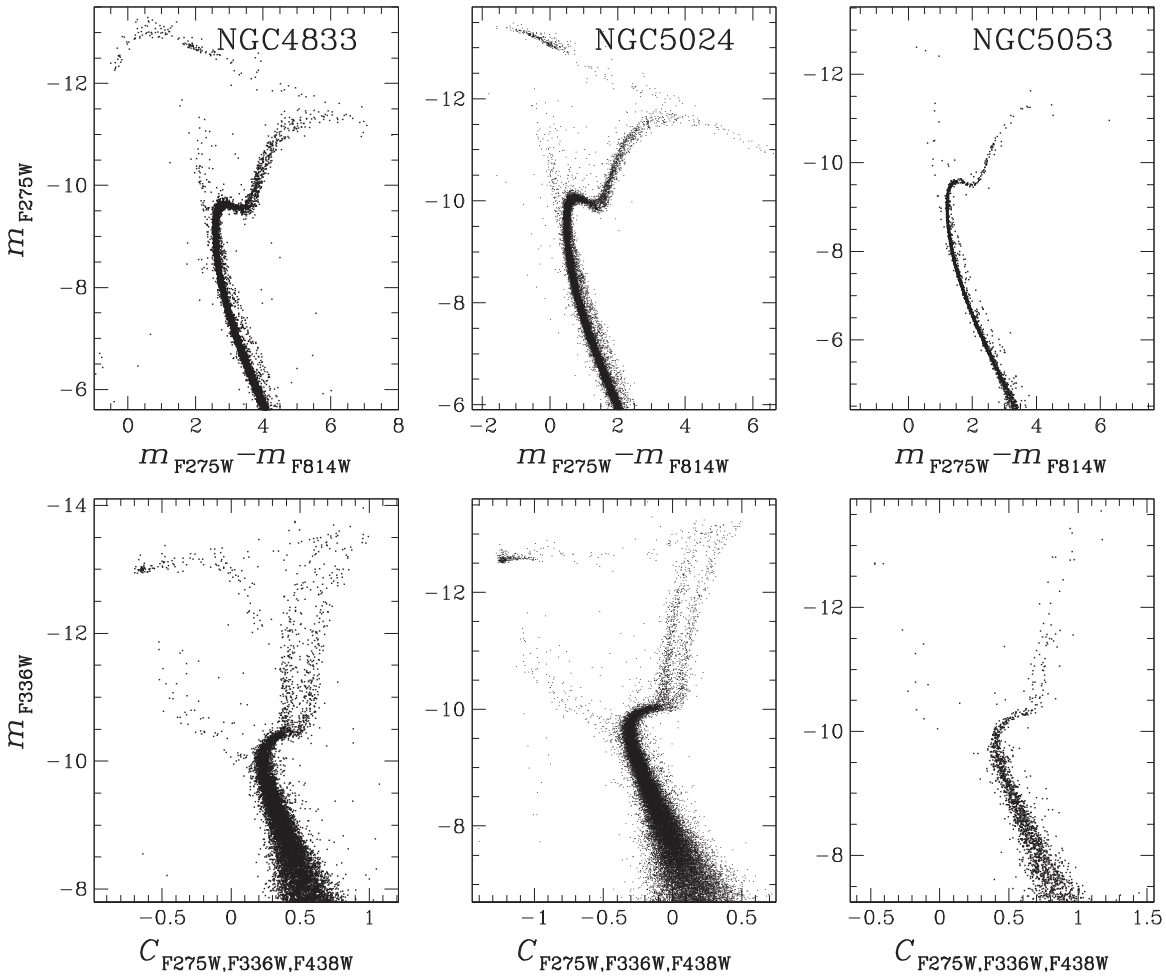

Figure 7. As in Figure 4, for NGC 4833, NGC 5024, and NGC 5053.

$m_{F275W} - m_{F336W}$ CMDs, 1G stars are redder than 2G ones, but they become bluer in the m_{F336W} versus $m_{F336W} - m_{F438W}$ CMDs (right panels).

Thanks to F275W, F336W, and F438W data, the two stellar generations are clearly distinguished and are seen to wind, in a distinct but intertwined fashion, from the MS through the subgiant branch (SGB) and RGB, to the HB.

The UV passbands are thus able to probe the CNO content of the cluster stars. Note that the nuclear processes that produce the light-element (anti-)correlations (e.g., the Na–O or the Mg–Al anticorrelations) also produce helium, and measuring the He enhancement of each sub-population is particularly important to help pinpoint what kind of stars may have produced the 2G material. The photometric impact of He is mainly on the optical bands (through the stellar temperature). After population-tagging stars according to their UV colors, we can make fine distinctions (~0.01 mag in color) in the MS ridge lines of the generations in the optical bands, and thus infer variations of only a few percent in He (Milone et al. 2010, 2012a, 2012b). In summary, the combination of UV and optical colors allows us to estimate the content of C, N, O, and He, even for stars that are far too faint to pursue with spectroscopy. (See Milone et al. 2012a, 2012b, 2013 for applications of the method.)

The combination of UV/blue filters that we have selected for GO-13297 is also ideally suited for studies of horizontal-branch stars (HB stars), blue stragglers stars (BSSs), and compact binaries. For hot HB stars, optical colors quickly become degenerate, but UV colors are able to follow the entire HB extension. This is particularly interesting for those GCs (even some metal-rich ones; Rich et al. 1997; Busso et al. 2007 Bellini et al. 2013a) that have very extended HBs and often exhibit the most complex MPs. Enhanced helium also distorts the HB morphology: when Y is increased from 0.23 to 0.38 the blue HB becomes 1 mag brighter in F275W, while the EHB becomes 0.5 mag fainter. Thus the UV band is crucial for determining the physical parameters of HB stars (including T_{eff}) and their helium content (Rood & Crocker 1989; D'Antona & Caloi 2008). BSSs, compact binaries, and high-energy sources are also best studied with filters of shorter wavelength.

3. THE NEED FOR A BROAD SURVEY

Detailed studies, made possible largely by *HST*, have revealed remarkable variety and complexity. As mentioned above, among the dozen or so GCs in which multiple photometric sequences have been resolved thus far, the fraction of 2G stars ranges from a few percent to well over 50%. Each GC has its own individuality, thus pointing to a great deal of variance in the formation process itself. Yet the sheer range of variance remains to be established, and cannot be properly mapped without the widest possible survey of Galactic GCs. Furthermore, since spectroscopy has shown that nearly all GCs

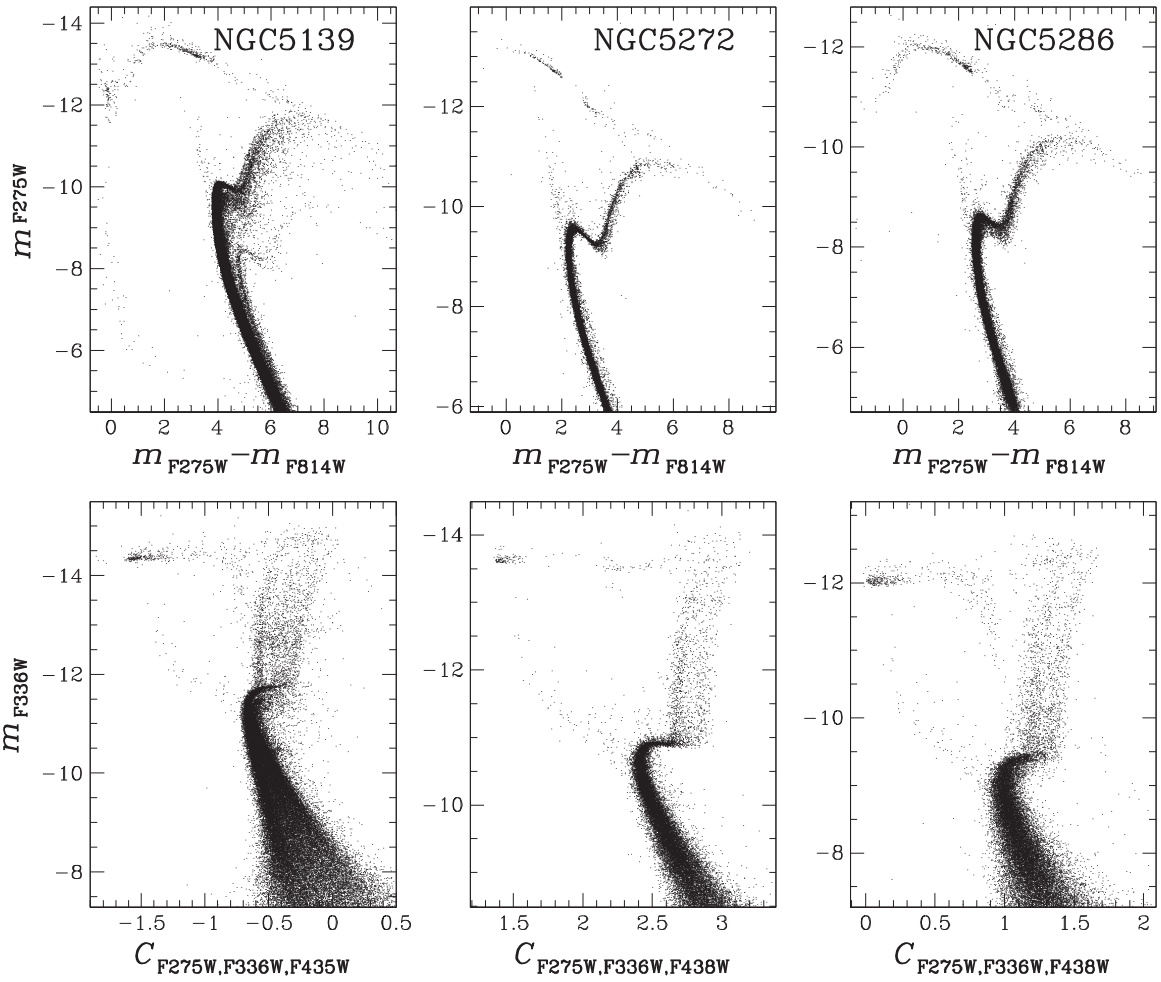

Figure 8. As in Figure 4, for NGC 5139, NGC 5272, and NGC 5286.

host MPs, it is all the more appropriate to move from studying a few "odd ducks" to a systematic survey of the whole flock.

The largest homogeneous set of *HST* data on GCs until now is the ACS Treasury database of F606W and F814W images for 65 GCs (GO-10775, PI Sarajedini, Anderson et al. 2008); however, its optical-wavelength baseline offers sub-optimal leverage for MP studies. The new GO-13297 data set represents what is needed: to augment the existing database with UV and blue observations through the "magic trio" of WFC3/UVIS filters, F275W, F336W, and F438W, whose power in population separation we have just illustrated. Our photometry will characterize the populations in each cluster: how many stellar generations are present, and in what relative proportions—even for small minority populations that might easily escape spectroscopic surveys. The UV/blue WFC3/UVIS photometry, combined with visible photometry from the ACS GC Treasury, will also enable a systematic survey and detailed intercomparisons of the populations of EHB stars, BSSs, and compact binaries in a large sample of Galactic GCs, as outlined in Section 8.

4. THE GC SAMPLE AND THE OBSERVING STRATEGY

Figures 1 and 2 show that MPs of many clusters can be readily disentangled by means of a two-color diagram made from F275W, F336W, and F438W. In order to effect a clean separation of the populations with the CMDs and the pseudo-color diagrams, our observational goal was a color precision of about 0.02 mag or better, which implies a signal-to-noise ratio (S/N) of 50 or better in F275W (the most photon-starved filter). We did not try to follow the multiple sequences all the way down the MS for every cluster—that would have been prohibitively expensive orbit-wise. Rather, our goal was simply to maintain this precision in F275W to just below the turn-off. That will naturally give us a population separation for the evolved populations as well.

Given that we need a minimum of four exposures in each band to make a robust catalog, two orbits represent the minimum set of observations for each cluster. 15 clusters are observed with that allocation (see Table 1 for a detailed description of the observing time allocated for each cluster and for the different filters). Four clusters need three orbits each, eight clusters need four orbits, three need five orbits, and two clusters need six orbits each. (One of the six orbit clusters is NGC 6715 [M54], which is too far away to get 0.02 mag precision below the turn-off in F275W. But it is likely to have a larger MS spread, and therefore not need an S/N as high as 50. Furthermore, understanding its upper sequences with an MP-sensitive filter system will be important.)

The remaining 14 clusters are so far away or so reddened that we cannot hope to resolve MS splits with F275W; for these

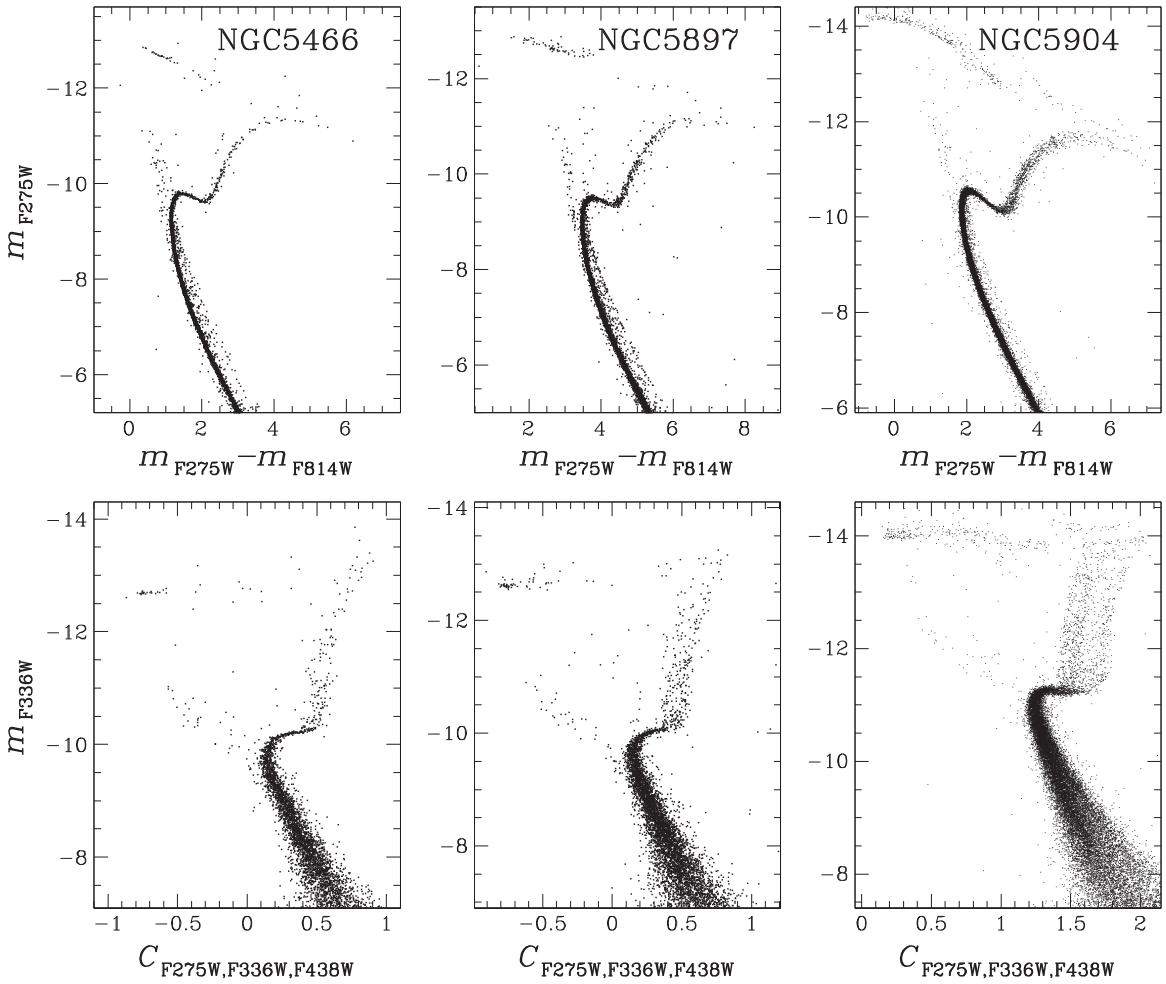

Figure 9. As in Figure 4 for NGC 5466, NGC 5897, and NGC 5904.

clusters we allot two orbits, which are adequate for the SGB, RGB, and HB populations.

We observe each GC in two visits, with orientations separated by roughly 90°, to allow a direct validation of the charge-transfer efficiency (CTE) corrections (see below). For most GCs, we take two exposures per filter per visit. These exposures are dithered to cover the gap, so that most stars will be found in four exposures in each band, thus allowing a robust empirical estimate of the photometric errors.

In summary (see Table 1), the GO-13297 GC sample includes 47 GCs and a very old (~8 Gyr, King et al. 2005) open cluster, NGC 6791, which has been included in the sample because of its many peculiarities (Bedin et al. 2008; Geisler et al. 2012). The program has been allocated 131 orbits. Originally, the program also included NGC 4147. Unfortunately, the cluster could not be scheduled (for guide-star problems) and has been substituted with M4. Before GO-13297 we had a pilot project, GO-12605 (PI Piotto, 22 orbits), where we began our collection of WFC3/UVIS F275W, F336W, and F438W images for seven GCs (M3, M13, M15, M80, NGC 288, NGC 362, and NGC 2808), extending previous F606W and F814W data from GO-10775. In an even earlier project, GO-12311 (PI Piotto, 17 orbits), we had collected WFC3/UVIS F275W images in the GO-10775 fields of five more clusters (47Tuc, M4, M22, NGC 1851, and NGC 6752). The GO-12311 data set is now complemented by F336W and F438W WFC3/UVIS images for NGC 1851, M4, and M22.

Some of the GCs from the previous GO-10775 Treasury program were not included in the GO-13297 target list either because they are too poorly populated for a meaningful search for multiple sequences, or because they are highly reddened or extremely distant, which would have made them impossible to observe in the UV in a reasonable number of orbits. In summary, completion of the GO-13297 program gives us, across all programs, 57 GCs with a homogeneous set of images in the five photometric bands F275W, F336W, F438W, F606W, and F814W.

Table 1 lists these 57 clusters and summarizes their WFC3/UVIS and parallel ACS images. The final five columns in the table give the Galactic *XYZ* coordinates, the reddening, and the distance modulus (from the Harris 1996 catalog, 2010 edition). GCs observed within GO-12311 are marked by an asterisk, GCs from GO-12605 by two asterisks. Figure 3 shows the distribution of the clusters in the Galactic *XY* and *XZ* planes.

WFC3/UVIS has been on board *HST* for only a few years, yet CTE losses have become a concern for it much more quickly than they were for ACS. The UVIS team has traced this to the fact that CTE losses are particularly bad when the background is low (see MacKenty & Smith 2012). In order to minimize CTE losses, we determined the anticipated background for each exposure and supplemented it with postflash to

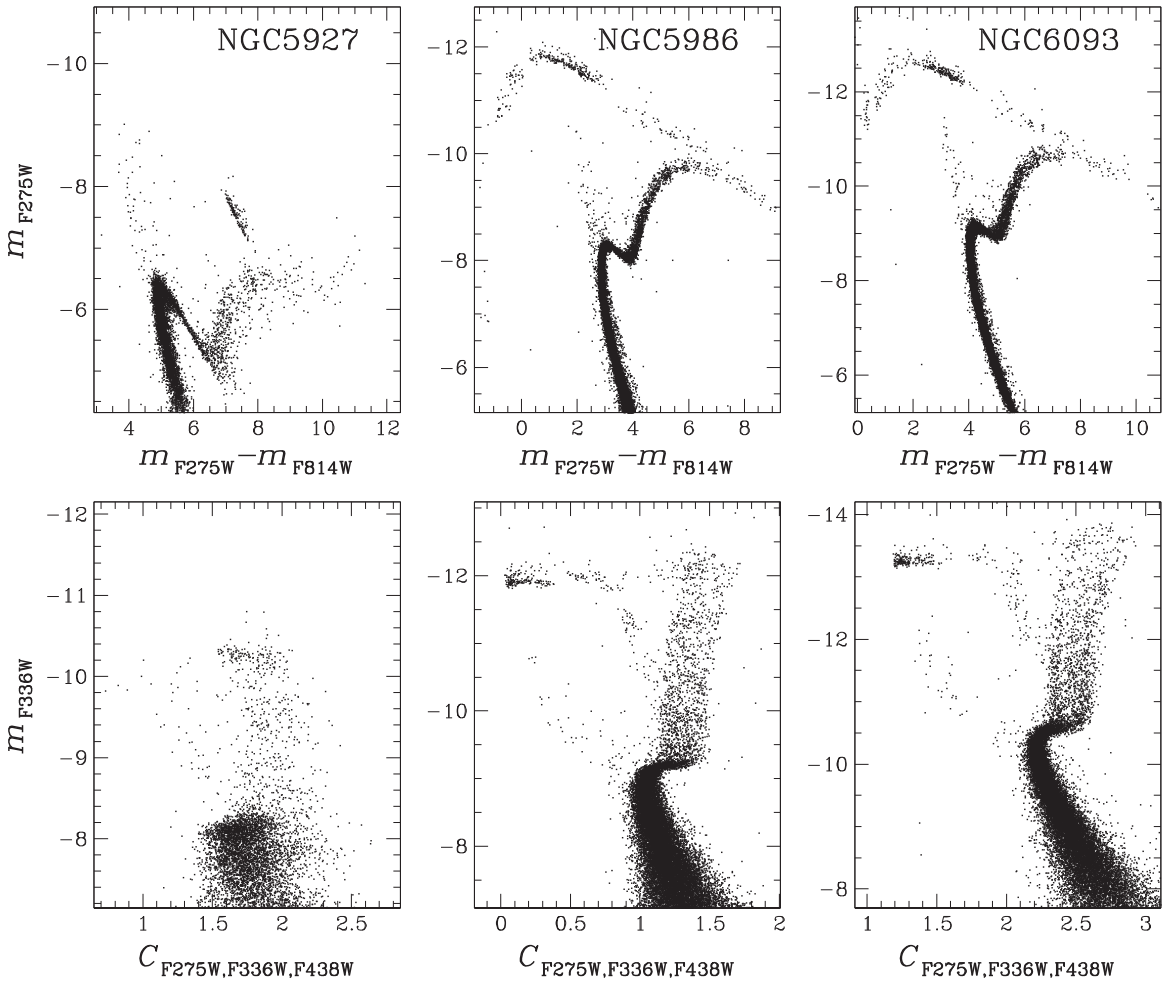

Figure 10. As in Figure 4, for NGC 5927, NGC 5986, and NGC 6093.

ensure a minimum of 12 e^-. In addition, to the extent possible, we observed each cluster at two different orientations 90° apart so that any remaining CTE issues could be dealt with properly. We postflashed our images to ensure a background of a least 12 e^-.

The main focus of our program is UV imaging of the central field of each cluster, and our observing strategy was optimized for that field. Even so, we could still afford to take ∼4 medium-length exposures of a parallel field with ACS (more for the clusters with more than two orbits). Our general strategy has been to take one orbit at one orientation and another at a different orientation. This resulted in placing the ACS/WFC camera on two different fields 6′ from the cluster center. For large He differences among the different populations, even these few parallel observations will allow us to detect split MSs, as was successfully done in the case of NGC 2808 (Piotto et al. 2007). The mapping of the outskirts of the clusters, albeit at lower photometric accuracy, adds a large baseline to the spatial aspects of our MP study, and will allow us to measure the 1G/2G radial gradient. The relative concentration of the 2G stars provides critical information about the formation process (see D'Ercole et al. 2008 and Bellini et al. 2009).

When possible, we have chosen an orientation that allows the parallel fields to overlap previous observations, so that we can also measure proper motions (PMs) for the outer field. At a minimum, we can use the WFPC2 parallels taken during the GO-10755 program, but many clusters have even better archival data. Note that the overlaps with previously collected GO-10775 images provide us with a ∼7 year temporal baseline for relative PM measurement. The outer-field observations should be deep enough to allow us also to measure absolute PMs for the clusters, relative to background galaxies.

5. DATA REDUCTION

The ultimate goal of this program is to provide comprehensive catalogs to the community in order to enable the many studies that this 57 cluster data set makes possible. It will not be possible to produce the best possible catalogs immediately. Once we have the entire data set in hand, we will be able to do an exquisite characterization of the point-spread functions (PSFs) and distortion solutions for each filter, as well as empirical corrections for any remaining CTE issues. Therefore the final catalogs will not be available until about a year after the last data are taken.

There are, however, many studies that will not require a definitive catalog, and we are making preliminary products available to the community as soon as possible. In addition, team members will be performing special processing on individual clusters to produce early science results.

We describe in the following subsections the three different reductions we envision for this project: the early-release

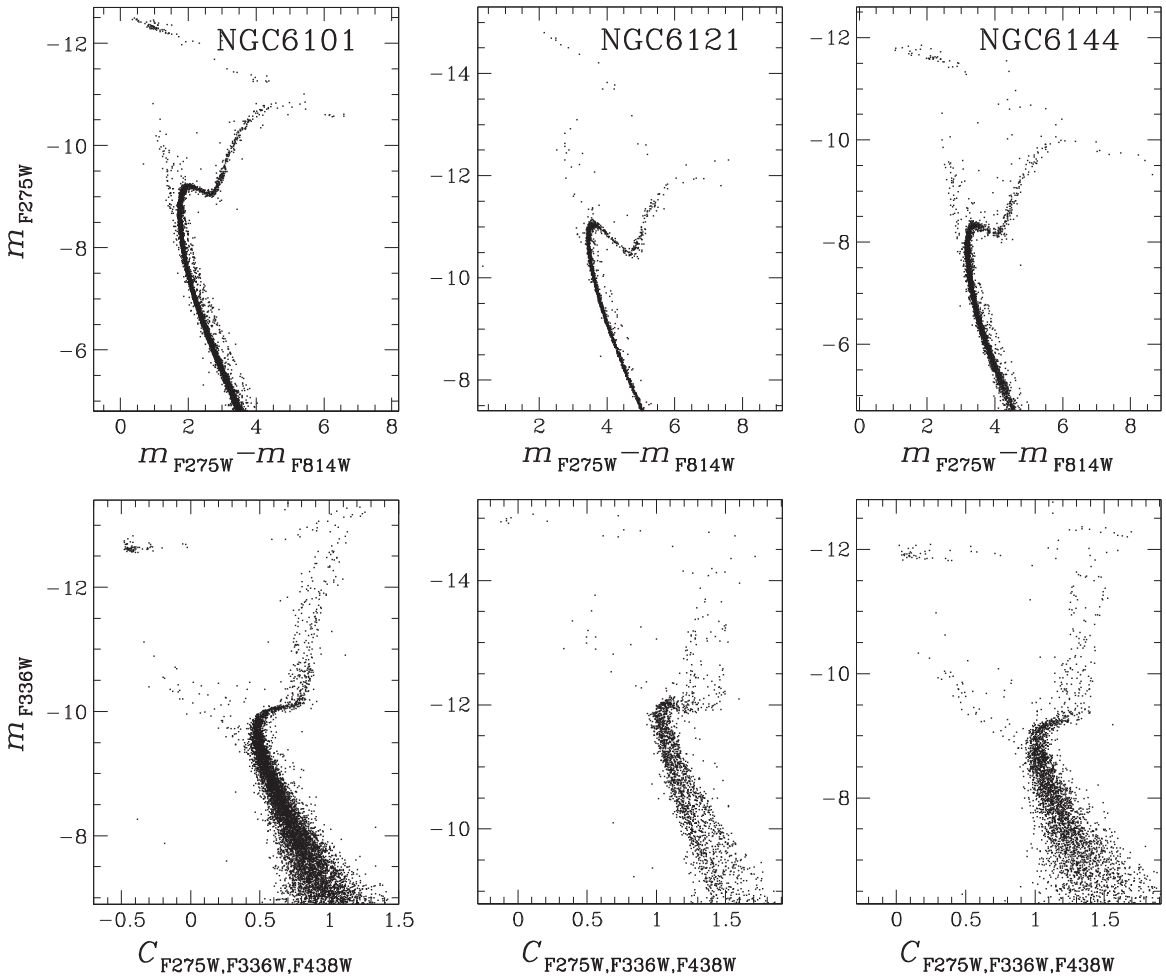

Figure 11. As in Figure 4, for NGC 6101, NGC 6121, and NGC 6144.

preliminary reduction, the specialized reductions for early science, and the final comprehensive reduction.

We have created a web page (http://groups.dfa.unipd.it/ESPG/treasury.html) where interested persons can follow the progress of the project and retrieve the released photometric and astrometric data. A mirror site will also be available in the MAST archive at STSCI.

5.1. Early-release Reduction

Much of the progress in understanding the MP phenomenon will be possible only by combining photometric observations of larger numbers of stars with targeted spectroscopic studies of individual stars. In an effort to allow spectroscopists to identify stars and plan their runs as soon as possible, we will provide an early reduction of the data shortly after the publication of this paper. We will update the archive as more data come in.

The preliminary reduction will focus on measuring the stars in the simplest way possible and collating them with the existing GO-10775 catalogs in F606W and F814W. To this end, we run on each exposure a version of img2xym_wfc3uv (similar to the one-pass star finding and measuring for ACS described in ACS/ISR-2006-01 by Anderson & King, but adapted to the WFC3/UVIS detector). This is a one-pass finding routine that goes through the image pixel by pixel, identifying as a potential star any pixel that has more than 100 counts within its inner 3×3 pixels and has no brighter pixels within a radius of 4 pixels. On each identified source we then use an empirical library PSF to perform PSF-based 5×5 pixel aperture photometry and determine an accurate position. Our procedure then uses the WCS information to transform the measured positions into the GO-10775 catalog frame and matches up each star list to the stars in the catalog.

Once this has been done for all the available exposures, we collate the observations of each star in each filter and produce a catalog that has the following elements: first, we provide a 2013–2014 position that can be compared against the 2006 position from GO-10775. Since we have not optimized the PSFs and astrometric transformations, this position has only 0.1 pixel precision, but that should be sufficient for cluster-field separation. We next provide the F275W, F336W, and F438W photometry for all the stars in the GO-10775 catalog that could be found by our one-pass routine. We provide the VEGA-mag-calibrated average magnitude, the rms deviation of the individual observations about this average, and the number of images that contributed to the average. Finally, we also produce stacked images in each of the three new bands, in the frame of the original F606W products.

5.2. Data Reduction for Early-science Papers

The early-release catalog described above has been constructed with a library PSF and a one-pass finding approach that treats each star as if it is isolated. The final reduction will

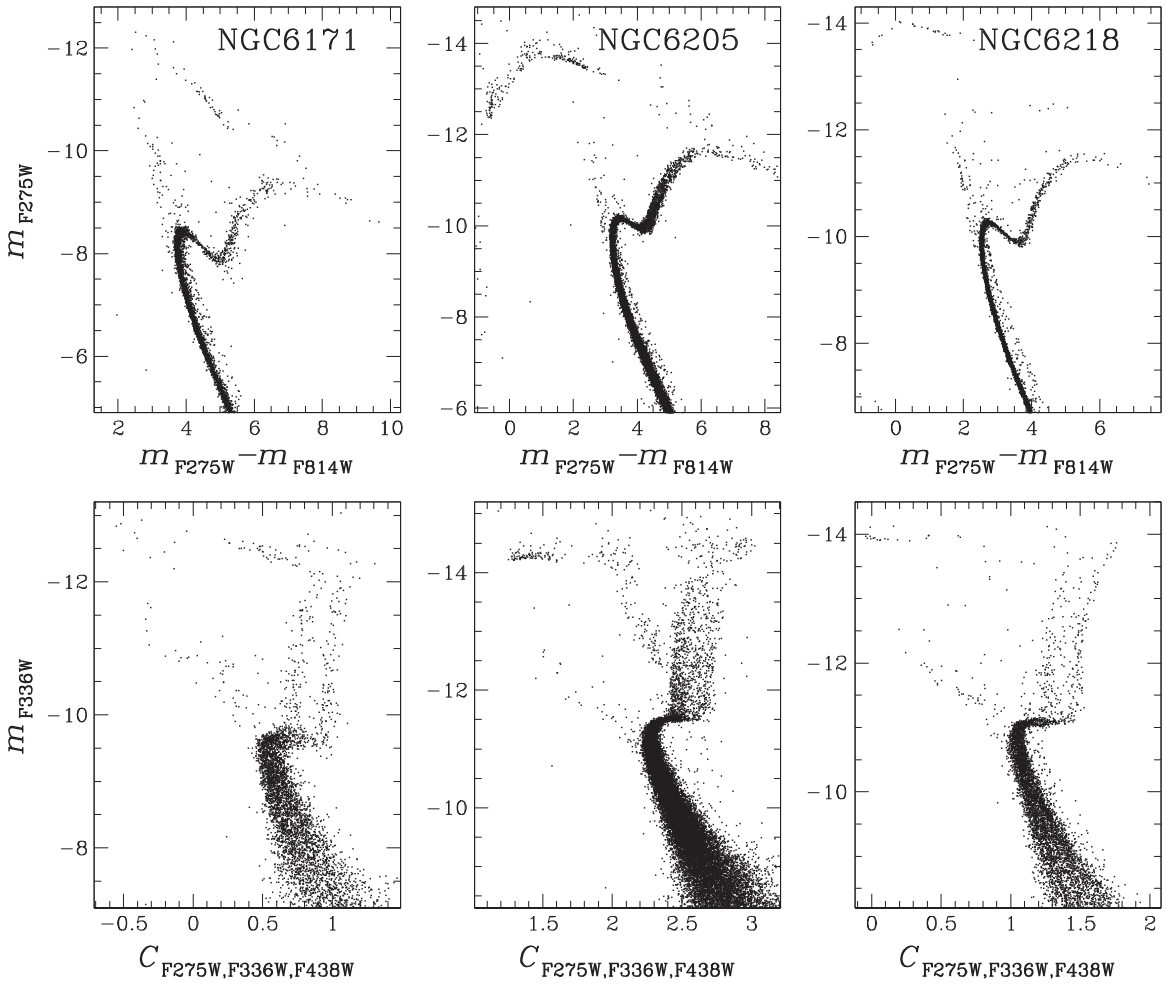

Figure 12. As in Figure 4, for NGC 6171, NGC 6205, and NGC 6218.

improve on several of these limitations, but since it will be more than a year before the final reductions are available, in the meantime several members of the team have been running supplemental reductions in order to start the detailed scientific analysis of several clusters.

These reductions will be described in more detail in the individual papers (for example, see Milone et al. 2015, Paper II, for M2), but many of them will make use of photometry software (such as that described in Bellini et al. 2010; Anderson & Bedin 2010) that allows for the fact that the PSFs in individual exposures often differ slightly from the library PSF. The specialized reductions will also include differential reddening corrections. Both of these improvements are necessary to enable the best possible sequence separation for study of the MPs.

Other early-science projects will focus on the internal PMs. The one-size-fits-all preliminary products will not do the careful transformations and multi-epoch fitting that is necessary to measure accurate motions and their errors. For the clusters of particular interest, we will reduce all the available epochs and explore the internal motions in papers before the final catalogs are available.

These data are available for specific projects under request to the first author of this paper, and will be stored on the dedicated web page at the Department of Physics and Astronomy, of the University of Padova (http://groups.dfa.unipd.it/ESPG/treasury.html). The preliminary photometry coming from this process is at the base of the CMDs we present in this paper.

5.3. Final Data Reduction

The final reduction for this program will be possible only after all of the data are collected. The full data set will enable us to construct an exquisite model of both the average PSF and the average distortion solution in each of the three filters. We will also construct a tailored PSF for each exposure to reflect the fact that breathing causes it to vary slightly from the average.

Whereas for the preliminary reduction (described in Sections 5.1, 5.2) we reduced each exposure separately with a simple one-pass approach and combined the star lists with the existing GO-10775 catalog, for the final reduction we will construct an entirely new catalog using an approach that analyzes all exposures simultaneously in a multi-pass, artifact-avoiding, neighbor-subtracting algorithm similar to that used to reduce the original GO-10775 data set (Anderson et al. 2008). This new approach will involve all five filters and will produce PMs, source-subtracted stacks (which anyone can search for remaining objects of any sort), and a variety of artificial-star tests.

In addition to reducing the GO-10775 and GO-13297 data in a uniform way, we will also reduce all of the existing WFPC2,

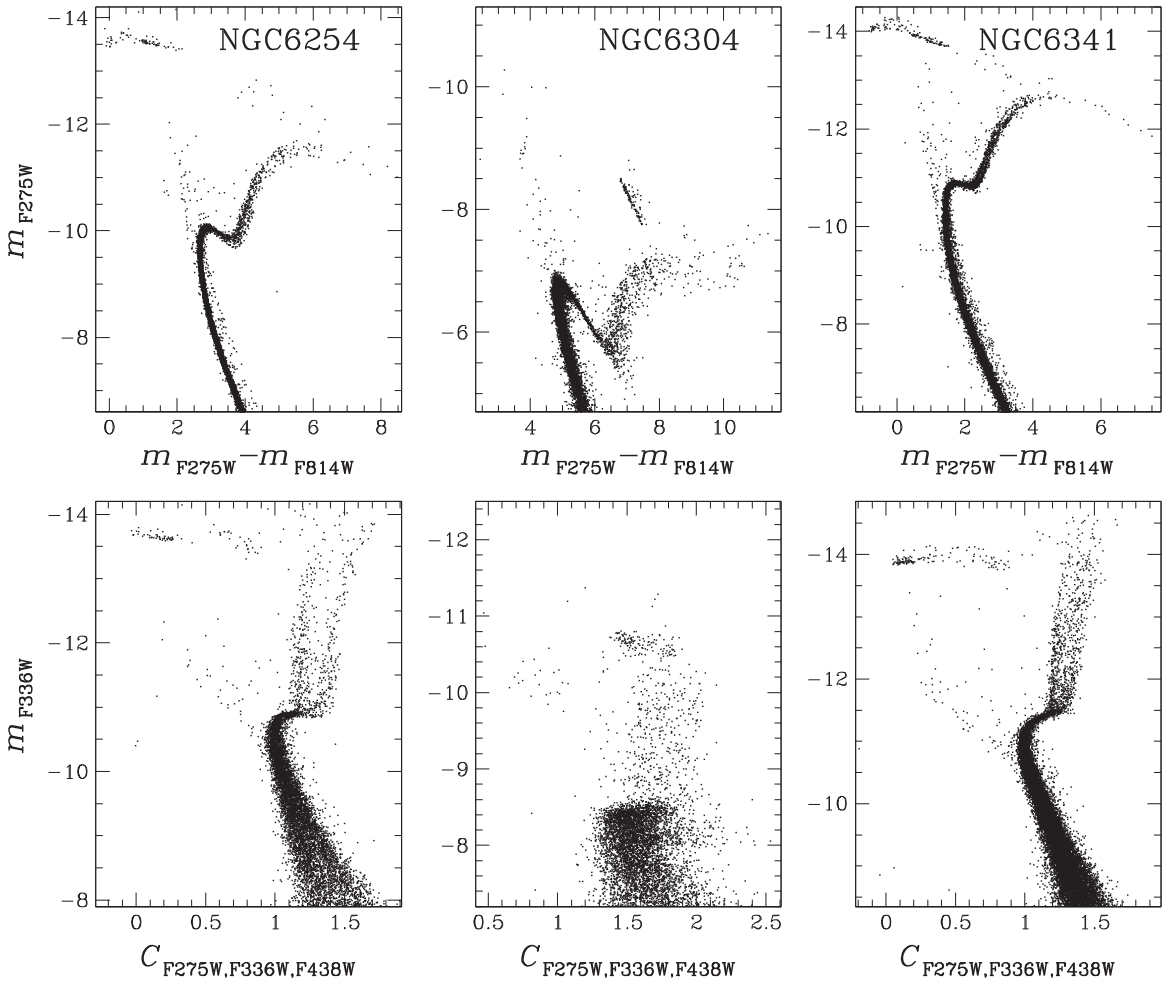

Figure 13. As in Figure 4, for NGC 6254, NGC 6304, and NGC 6341.

ACS, and WFC3 data for the clusters and cross-identify the stars with our catalog, producing time-series photometry and astrometry that can be used for high-precision PMs and variable-star studies. From these many individual observations of each star, we will measure a variability index and a high-precision PM, along with an error estimate of the latter. Along with each photometric observation, we will also provide a differential-reddening correction, so that accurate CMDs can be constructed for multi-population analysis.

6. HIGH LEVEL PRODUCTS

6.1. Preliminary Release of Astrometry, Photometry, and Proper Motions

The data products described in Section 5.3 (the new F275W, F336W, and F438W photometry for the GO-13297 star catalog and new stacked images) are being made available via the http://groups.dfa.unipd.it/ESPG/treasury.html web page and the STSCI MAST archive (via the high-level product link in the archive listing for the proposal). We will continually update the files as new observations come in.

6.2. The Final Catalogs

Once all the data are in hand, we will perform the specialized uniform reductions described in Section 5.3. In addition to outputting those reductions we will also produce for each cluster several other high-level products.

1. A unified star list for the central field for all filters. We will have at a minimum F275W, F336W, F438W, F606W, and F814W for all clusters. We will also link up other relevant photometry from other archival data, such as SBC and FUV WFPC2 observations, which are particularly relevant to hot populations. For each filter, we will provide an average flux and its error, based on internal agreement. We will also provide the flux measured for each star in each exposure so that users can search for variability.
2. A differential-reddening map for each cluster, and a correction for each measurement of each star.
3. PMs for most of the stars in the catalogs. These motions will be focused on the UV data set, so they will extend from the brightest giants to a few magnitudes below the turn-off, so that they will be particularly useful for comparison with radial velocities and spectra from the ground.
4. Artificial-star tests done for stars inserted along the fiducial sequences. This will allow users to quantify the extent to which crowding may broaden the sequences.
5. Stacked images of the field in all filters, co-registered and with 2MASS-calibrated WCS headers. This includes data sets from the archive and any other data we can link-up

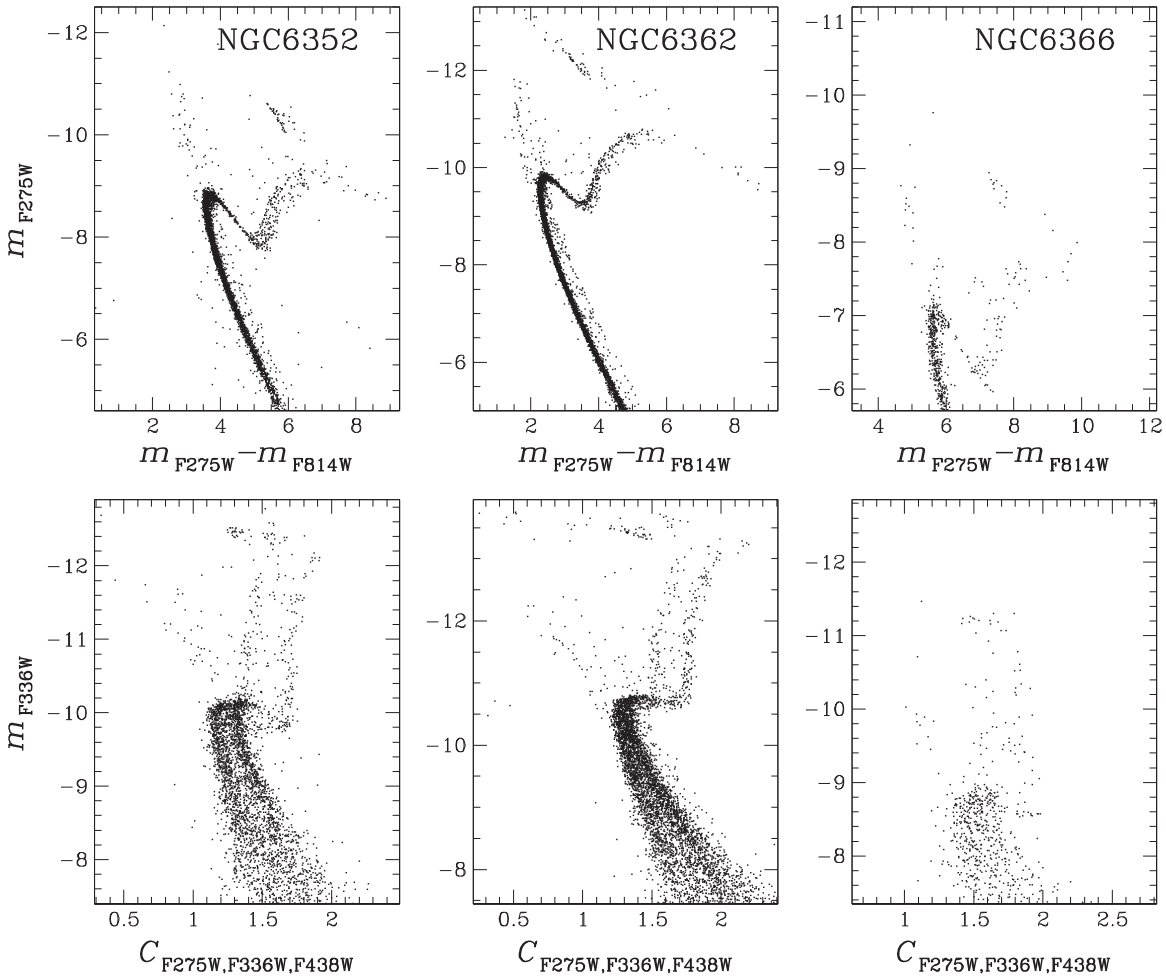

Figure 14. As in Figure 4, for NGC 6352, NGC 6362, and NGC 6366.

(including *Chandra* images). We will also provide subtracted stacks so that the community users can determine whether there might be any stars that escaped our finding algorithm.

6. A specialized website portal to serve up the data in a way that is most useful to GC researchers. It will allow users to zoom in and out of images and select stars for dynamic display on CMDs and PM diagrams. Stars will be flagged by evolutionary stage and 1G/2G designation. We will also indicate which stars have spectra available in the archive that we will maintain. We will, of course, also deliver our catalogs and images to MAST for a more standard dissemination.

While there is much science we are eager to do on this data set, the primary focus of the program is the generation of a legacy data set for the entire community. That is why we are providing the preliminary reductions as quickly as possible, and are equally intent on getting the final high-level products to the community within a year of the last observation.

7. FIRST COLOR–MAGNITUDE DIAGRAMS

At the time of the submission of the present paper, about 95% of the GO-13297 observations have been collected. Though it will take some time before we can perform the final reduction as described in Section 5.3, we are constantly monitoring the data acquisition, and all data are reduced following the procedures described in Section 5.2. A more detailed analysis of the multiple stellar population for some specific, particularly interesting clusters is ongoing, and corresponding papers will be submitted in the next few months. Here, we want to make public the first CMDs as they come out from our preliminary photometry. The data reduction process is still ongoing, and the purpose of the CMDs we are presenting here is just to show the potentiality of the GO-13297 database.

In Figures 4–23 we present the F275W versus $C_{F275W,F336W,F438W}$ and the F275W versus F275W – F814W diagrams. Magnitudes are instrumental magnitudes. Instrumental magnitudes are defined as the $-2.5\ \log_{10}$ of the sum of the detected photo-electrons within a circular aperture of 10 pixels, in the reference exposures of each filter, chosen as the one with the longest exposure time. A careful calibration will need an appropriate aperture correction tailored to the adopted PSFs, which differs frame by frame. We will eventually do so, but, at the moment, in order to avoid future confusion, we prefer to show the CMDs using the instrumental magnitudes as defined above. The figures show the diagrams for the GO-13297 clusters observed (even partially, i.e., not all orbits collected) by 2014 August. The figures also include the CMDs from the two pilot projects GO-12605 and GO12311. More specifically, F275W, F336W, F438W data for NGC 288,

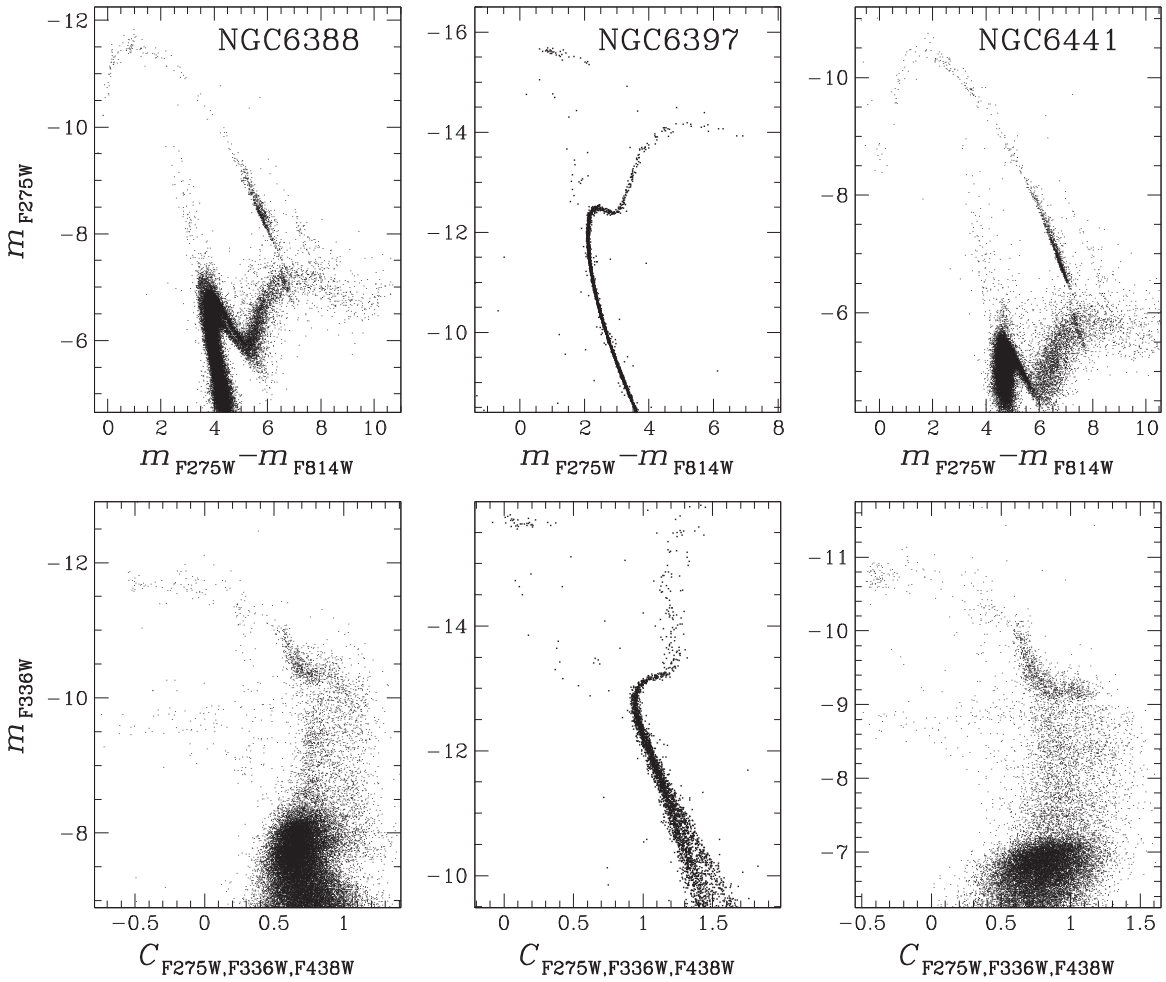

Figure 15. As in Figure 4, for NGC 6388, NGC 6397, and NGC 6441.

NGC 362, NGC 5272, NGC 6093, NGC 6205, and NGC 7078 come from GO-12605. F275W photometry for NGC 104, NGC 1851, NGC 6121, NGC 6656, and NGC 6752 is from GO-12311. Additional F275W and F336W data for NGC 104 and NGC 6752 come from the *HST* archive (see Milone et al. 2012a, 2012b for details). The F814W photometry comes from Anderson et al. (2008) and is based on GO-10775 data. F814W photometry for NGC 6791 comes from GO10265 archive data. For completeness, we also added the CMD of ω Cen from Bellini et al. (2010).

The CMDs are based on a preliminary selection of the best measured stars. There are margins for improved photometry and more complete star counts. A detailed analysis of the individual CMDs is beyond the purposes of this paper and will be deferred to future papers. Still it seems appropriate to emphasize that all GCs in this sample show multiple sequences or at least broadened sequences. This confirms the idea that the presence of multiple stellar populations in GCs is a widespread phenomenon, with single-stellar-population GCs being an exception (if, indeed, single-stellar-population GCs exist at all).

8. GO-13297 PROJECT LEGACY

The central theme of the GO-13297 project is to explore as fully as possible the MP phenomenon in GCs, which is clearly the key to understanding star formation and feedback in the cluster environment. However, our database will become a gold mine for a large number of other projects and will be a general resource for decades to come. In the following, we briefly describe the research projects our group intends to carry out using the GO-13297 astrometric and photometric database.

8.1. The Identification of Multiple Stellar Populations

This is of course our main goal. We will search for MPs in all evolutionary branches, in all clusters, following the procedure described in Milone et al. (2013) for NGC 6752, and in Milone et al. (2012a, 2012b) for 47Tuc and NGC 6397. The different populations will be chosen via different combinations of the photometry from the five bandpasses. We will do this by selecting individual stars belonging to different photometric sequences and calculating all their colors from combining the various passbands. In the final catalog each star will be assigned to a particular sub-population, in order to enable spectroscopic follow-up aimed at a precise chemical tagging of each sub-population. The catalogs and finding charts resulting from this effort will allow the entire community to contribute to this critical aspect of MP studies.

8.2. Modeling Multiple Stellar Populations

The peculiarities characterizing the chemical properties of the various sub-populations hosted by Galactic GCs require the

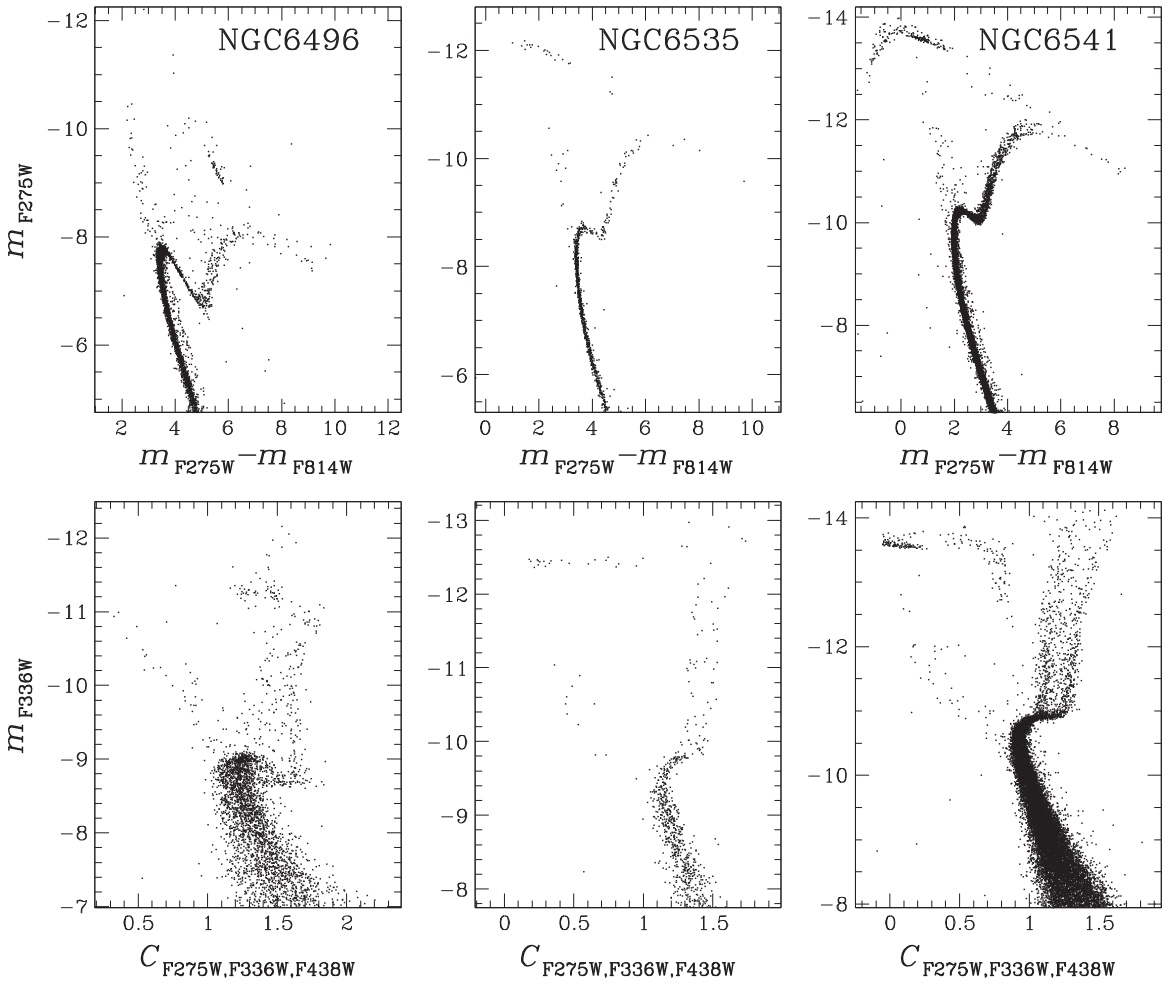

Figure 16. As in Figure 4, for NGC 6496, NGC 6535, and NGC 6541.

computation of extended sets of models for low-mass stars properly accounting for these chemical anomalies. This is a crucial step in order to investigate and trace the distribution of the distinct sub-populations in the various evolutionary sequences in the CMD from the faintest portion of the MS (Milone et al. 2012a, 2012b) to the HB (D'Antona & Caloi 2008; Dalessandro et al. 2011, and references therein). The photometric appearance of MPs strongly depends on the adopted photometric bands (Sbordone et al. 2011; Cassisi et al. 2013). In particular, since light-element anti-correlation strongly affects the stellar spectra at wavelengths shorter than 400 nm, when using UV and far-UV passbands it is crucial to use appropriate color–$T_{\rm eff}$ relations properly accounting for the various chemical anomalies. Basically, we will follow the method described in Milone et al. (2013, and references therein).

8.3. Measurement of He Content from Multiband Photometry

Multi-wavelength photometry provides unique information on the chemical composition of large samples of stars belonging to the different stellar populations hosted in GCs. As described in Section 2, the combination of filters centered at different wavelengths allows us to discriminate between various effects, like differences in He, C, N, O, Na content. Exploiting the sensitivity of various colors to different properties of stellar populations and combining the photometric information with grids of synthetic spectra constructed with chemical compositions constrained from spectroscopic observations will allow us to better isolate the specific role of the helium abundance. This technique has been successfully applied to a few GCs, and differences in helium among different stellar populations have been measured in 47 Tuc, NGC 6397, NGC 288, and NGC 6752 (Milone et al. 2013, and references therein). We plan to extend these measurements to the whole sample of clusters observed for this survey. The knowledge of the He variations within a GC will be used to extend the investigation on how this observable impacts the second parameter on HB morphology (see Milone et al. 2014b).

8.4. Cluster Structural Parameters from Star Counts

The appropriate combination of the UV-survey data and complementary wide-field observations will allow us to construct a new generation of GC radial star density profiles based on resolved star counts (see Ferraro et al. 2003a; Miocchi et al. 2013). This is indeed the most robust and reliable way to derive cluster structural parameters, since surface brightness can be biased by the presence of sparse, bright stars. This database will allow a complete re-characterization of the structural and dynamical properties of GCs.

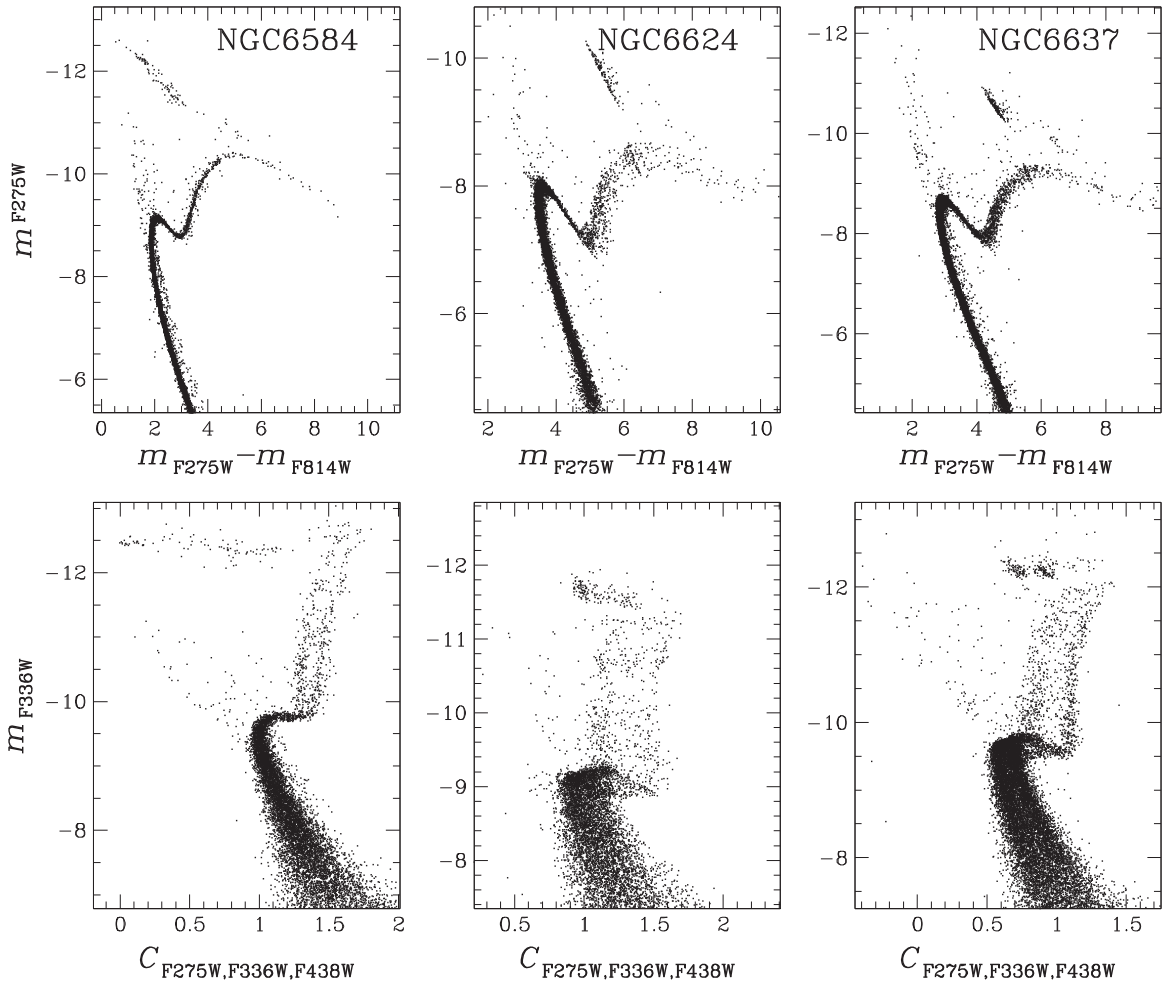

Figure 17. As in Figure 4, for NGC 6584, NGC6624, and NGC 6637.

8.5. Internal Proper Motion Analysis

Bellini et al. (2014) recently compiled the first large sample of GC PM catalogs using heterogeneous data from the *HST* Archive (see also Bellini et al. 2013b). This has shown that it is possible to reach the level of precision and accuracy required to study in detail the internal PM kinematics of GCs. Among other things, this will allow us to measure separately the kinematical properties of each of the different stellar populations photometrically identified (as in, e.g., Anderson & van der Marel 2010; Richer et al. 2013). Each GC observed as part of our GO-13297 program was also observed in 2006 by the GO-10775 Treasury program. Moreover, a good fraction of these GCs was also observed by other *HST* programs (in particular using the state-of-the-art detectors that have been available on *HST* since 2002). This will allow us to measure exquisite PMs with time baselines between 7 and 14 years. This will extend the work of Bellini et al. (2014) to a larger number of clusters, higher PM accuracy, and bluer stars. Among other things, this will allow us to measure separately the kinematical properties of each the different stellar populations photometrically identified. Any kinematical differences thus identified would strongly constrain formation mechanisms for the MP phenomenon.

8.6. Internal Dynamical Model and Central Intermediate-mass Black Holes

The new PM catalogs to be derived from our data will allow several new state-of-the-art studies of GC dynamics. For example, we will obtain direct measurements of the radial velocity dispersion profiles, the velocity dispersion anisotropy, and possible rotation of many GCs. Dynamical modeling will constrain the mass profiles of the GCs, including the possible presence of intermediate-mass ($\approx 10^3$–$10^4\,M_\odot$) black holes (van der Marel & Anderson 2010). The existence of such black holes continues to be debated in the literature (e.g., Noyola et al. 2010; Lanzoni et al. 2013; Lützgendorf et al. 2013), but this can be tightly constrained using PMs measured in the central arcseconds of the cluster. We will also be able to measure the velocity dispersion as a function of MS mass, and this will allow us to establish the extent to which GCs are in energy equipartition (Trenti & van der Marel 2013).

8.7. Absolute Proper Motions Based on an Extragalactic Reference Frame

Where possible, in our observing strategy we chose an orientation that allowed the parallel fields to overlap previous observations, so that we can also measure PMs in the outer fields. At a minimum, we can use the WFPC2 parallels taken

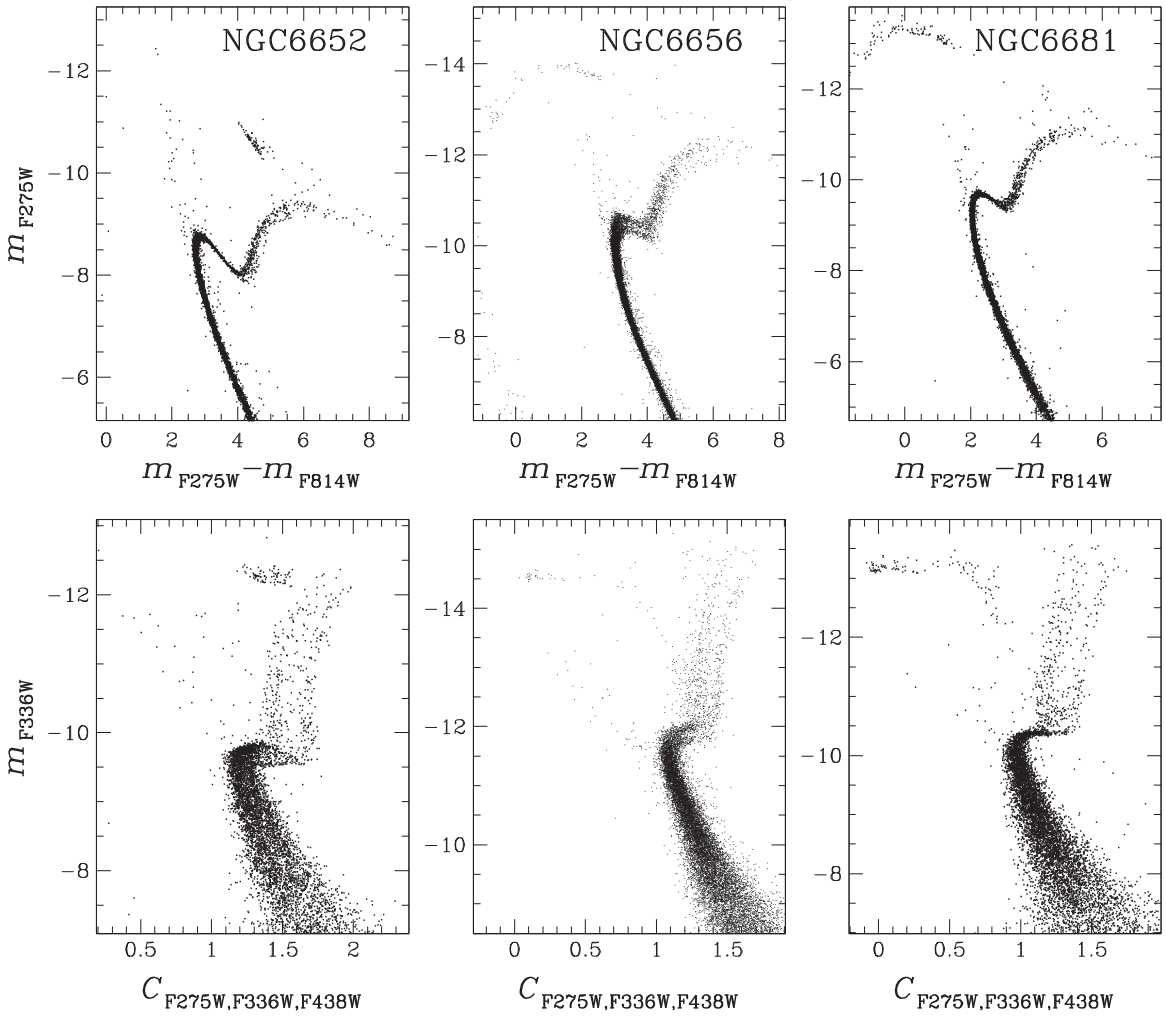

Figure 18. As in Figure 4, for NGC 6652, NGC 6656, and NGC 6681.

during the Sarajedini program, but many clusters have even better archival data. The outer-field observations are generally deep enough to allow us to measure absolute PMs for the clusters with respect to background galaxies. The central fields will be observed in UV/blue filters, so although we will explore them, we do not expect to find many background galaxies bright enough to be used as absolute points of reference.

Absolute PMs will be combined with radial velocities from the literature or from measurement of archival spectra, to derive the space velocities of the clusters; the position–velocity phase space will then be examined for possible groupings of clusters with similar multiple stellar population properties.

8.8. Parallel Fields and Ground-based Ancillary Data for the Radial Distributions of Multiple Stellar Populations

Astro-photometric catalogs and atlases in each of the filters will be electronically provided, also for the ACS parallel fields. When possible, PM membership and a sub-population flag will also be provided. Ground-based wide-field multiband photometry is already available for a large number of the target clusters. Merging ground-based with the new *HST* data will help connect stellar populations in the cluster centers with those in the external regions by using similar color combinations ($C_{U,B,I}$ is analogous to $C_{F275W,F336W,F438W}$), and therefore investigate their radial distribution. Moreover, identifying stars with available high-resolution spectra will allow us to connect photometric and spectroscopic properties of the different stellar populations. Observations with ground-based facilities (typically 8–10 m size telescopes) have already been acquired, and additional observations requested for a subsample of the GO-13297 clusters.

8.9. Modeling the Radial Distribution of Multiple Stellar Populations

Theoretical models and simulations predict that 2G stars should initially be more concentrated than 1G stars (see, e.g., D'Ercole et al. 2008; Bekki 2011; Bastian et al. 2013b, and references therein), and that many clusters should still preserve, at least in part, some memory of the initial differences in the 1G/2G spatial distribution (Vesperini et al. 2013; for observational studies that show radial gradients in the fraction of 2G stars see, e.g., Sollima et al. 2007; Bellini et al. 2009; Lardo et al. 2011; Milone et al. 2012a). We will carry out a systematic observational and theoretical study aimed at addressing a number of key questions concerning this issue. By studying the presence and extent of radial gradients in clusters with different dynamical properties and at different phases of their dynamical evolution we will be able (a) to further test the general validity of models predicting the initial spatial segregation of the different stellar populations, (b) to make progress in the

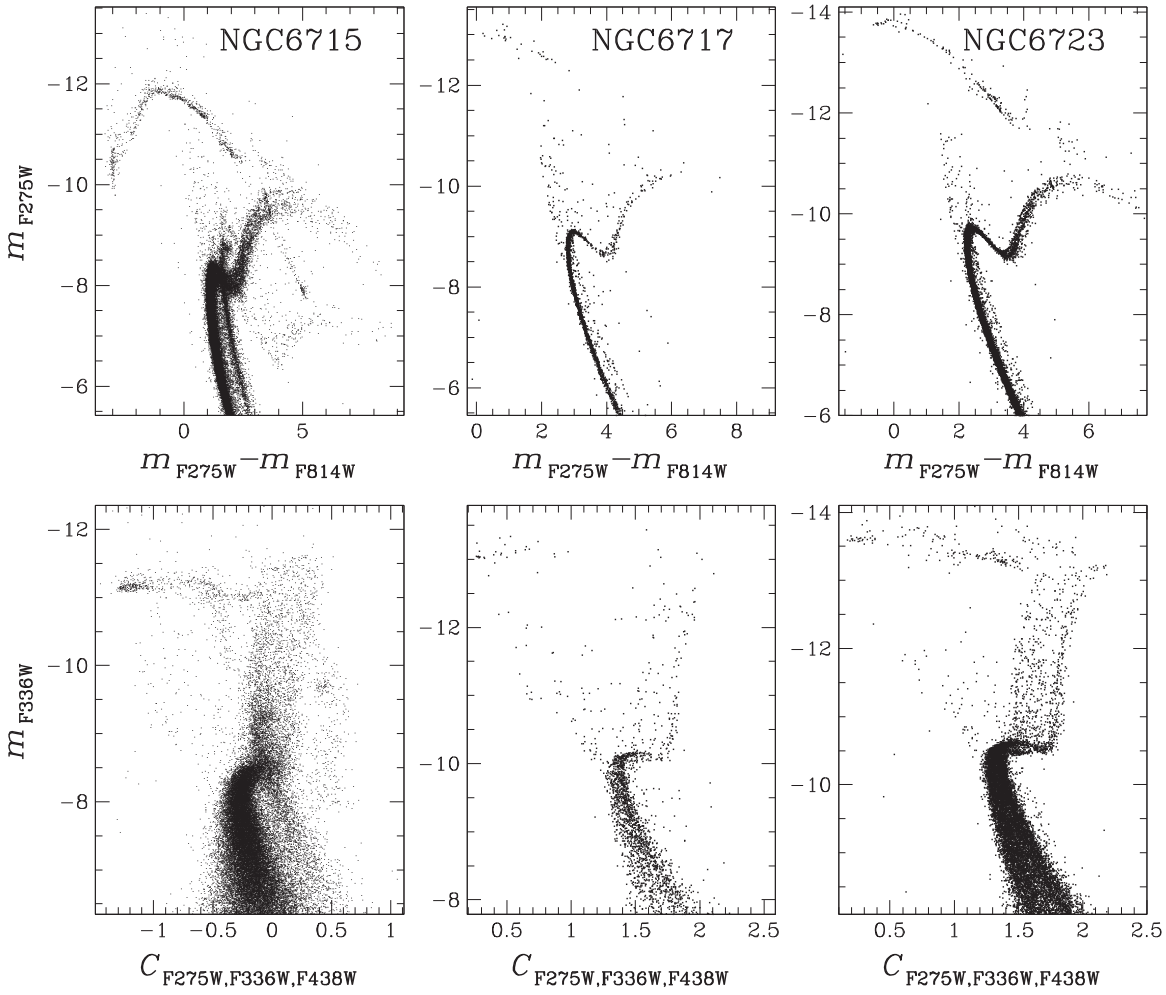

Figure 19. As in Figure 4, for NGC 6715, NGC 6717, and NGC 6723.

observational identification of an evolutionary sequence in the spatial mixing of 1G and 2G stars, and (c) to shed light on the relationship between the global 2G fraction and its local value measured at different distances from the cluster center.

8.10. Distances

Knowing the distances to Milky Way GCs is fundamental for several astrophysical fields, including stellar evolution, cluster dynamics, and the cosmological distance ladder. To date, GC distances have generally been obtained mostly through isochrone-fitting techniques and the RR Lyrae variables. By comparing high-precision *HST* PMs (at the level of mas yr^{-1}) with existing line of sight velocity data (in km s^{-1}), it becomes possible to obtain entirely independent kinematical distance estimates (either from the assumption of velocity isotropy or from detailed dynamical models). Such a study is currently in progress (L. Watkins et al. 2015, in preparation) using the PM catalogs of Bellini et al. (2014). With the new PM catalogs to be derived from the GO-13297 data, we plan to extend this work to a larger number of clusters and higher distance accuracies. These distances will be completely independent from, and in some ways complementary to, GAIA measurements.

8.11. RGB Bump

We plan to measure the RGB bump brightness and its extension in magnitude of the various sub-populations hosted by each cluster in our sample. Comparison with models will allow us to estimate He abundance differences among them. These differences can be compared with the He abundance measurements obtained with other methods (see previous sections). At the same time, the relative brightness of the RGB bump with respect to other CMD features, such as the HB luminosity and the MSTO, will provide useful tests for stellar evolution models (e.g., Cassisi et al. 2011).

8.12. HB Morphology

Because optical colors become degenerate at high temperature, our use of UV bands will enable an accurate characterization of the full HB morphology, including the extreme horizontal branch (EHB). The HB morphology will yield additional insight into any sub-populations enhanced in helium. At higher *Y*, the HB generally extends to hotter temperature, and also exhibits significant variations in luminosity, with higher luminosity on the blue HB and lower luminosity on the EHB. It will also be possible to establish to what extent the long-standing issue of the "second parameter" can be accounted for by helium-enriched second generations. Some of us have already shown that the multi-modal HB of NGC

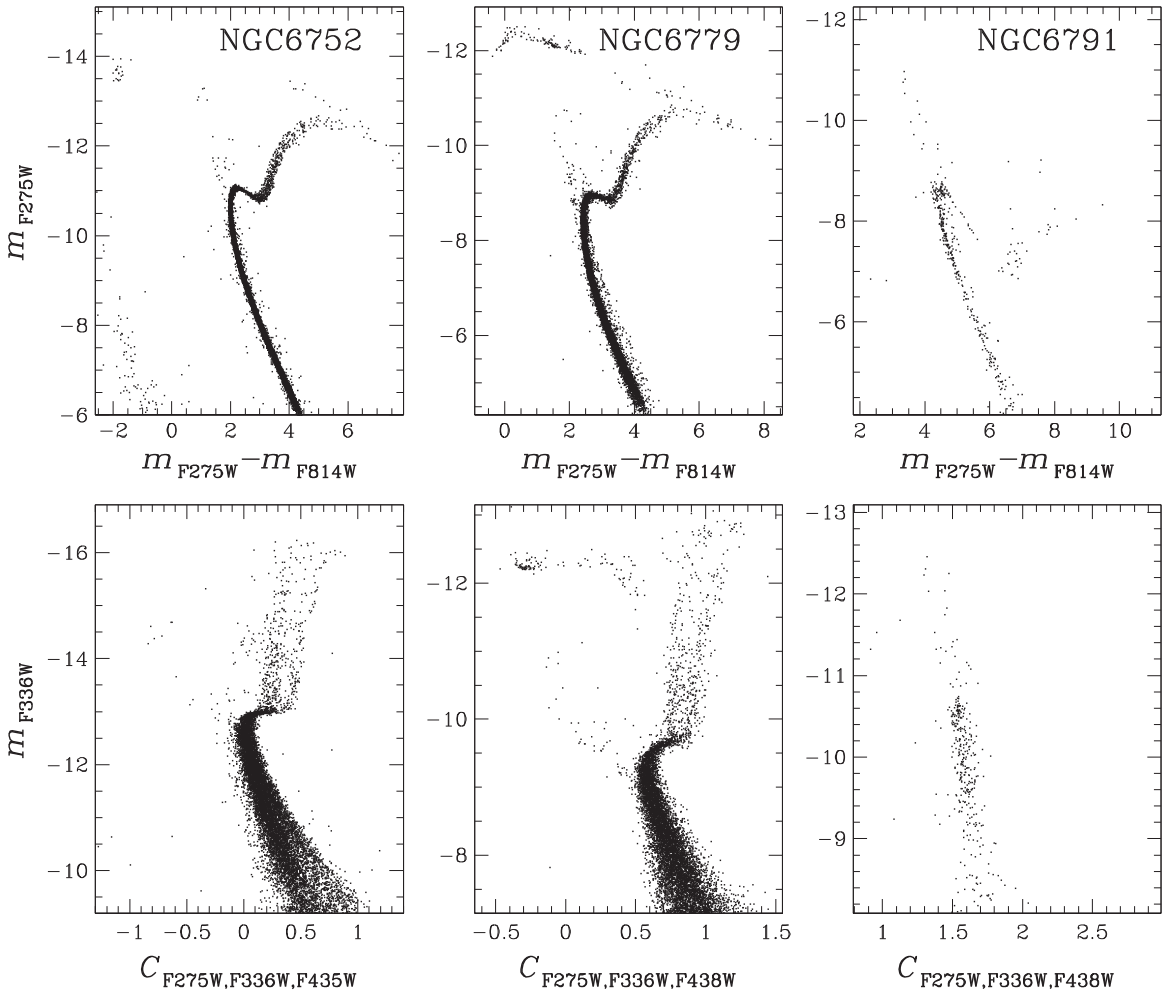

Figure 20. As in Figure 4, for NGC 6752, NGC 6779, and NGC 6791.

2808 (D'Antona & Caloi 2004; Dalessandro et al. 2011), as well as of the metal-rich GCs NGC 6388 and NGC 6441 (Busso et al. 2007; Caloi & D'Antona 2007; Bellini et al. 2013a), is consistent with multiple stellar populations with different helium abundance. This connection is supported by recent studies, based on spectroscopy of HB stars, which have shown that distinct stellar populations, with different content of light elements and helium, occupy different regions along the HB (Marino et al. 2011a, 2013, 2014; Villanova et al. 2012; Gratton et al. 2011, 2012, 2013). Additional examples of the possible effects of helium enhancement on the HB morphology for many other clusters can be found in Brown et al. (2010) and Dalessandro et al. (2013a). With the new GO-13297 we can extend the investigation of Milone et al. (2014b) on the nature of the GC global and local parameters and their effect on the HB morphology.

8.13. Modeling HBs

The HB morphology is very sensitive to the main parameters of the MPs, and in addition, to mass loss on the RGB. We need to build synthetic HBs, based on the computation of large grids of models, to check and quantify the role of all the parameters. New grids are being computed, including models populating the highest $T_{\rm eff}$'s of the HB. These structures are the outcome of "late helium core flash" ignition (D'Cruz et al. 1996; Brown et al. 2001). A crucial outcome of the comparison with observations will be to verify whether the very hot HB stars result from a high-helium population. As a by-product of the population synthesis for the HB, we also predict how large a population of helium white dwarfs is expected in clusters hosting extreme HB stars, as found by Bellini et al. 2014 in ω Cen.

8.14. Analysis of RGB + HB + AGB Star Counts (Searching for AGB Manqué Objects)

Spectroscopic studies have revealed that the AGBs of some GCs host only CN-weak/Na-poor stars, at odds with what is observed along the RGB, where both CN-weak and CN-strong stars are present (e.g., Norris et al. 1981; Pilachowski et al. 1996; Campbell et al. 2010, 2013). This has been interpreted as the presence of multiple stellar populations with different nitrogen and helium abundances. The helium-rich/nitrogen-rich stars would populate the hottest part of the HB, and then evolve without ascending the AGB, thus making the AGB populated by CN-weak stars only (Norris et al. 1981). We plan to analyze star counts of RGB, HB, and AGB stars to further investigate the connection between other stellar populations and AGB-manqué objects.

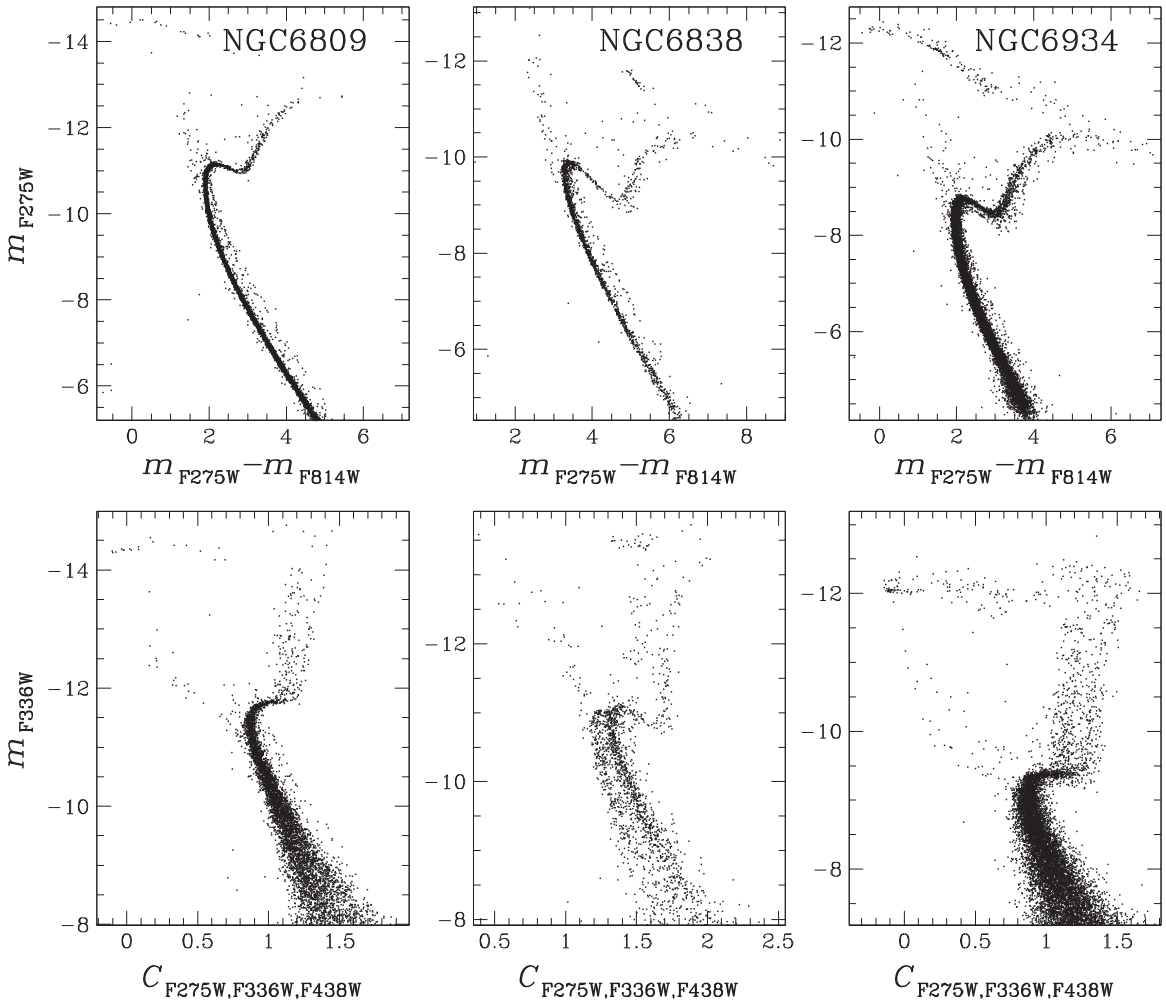

Figure 21. As in Figure 4, for NGC 6809, NGC 6838, and NGC 6934.

8.15. Globular Cluster Ages

Relative ages of 64 GCs were measured in the ACS Treasury Program of Galactic GCs (Marín-Franch et al. 2009). Single stellar populations were assumed, however, and no dependence on chemical abundances was taken into account; these limitations were due to lack of composition-dependent stellar-evolution libraries and to having only two-color photometry. The GO-13297 data set now adds three more UV/optical bands, and the resulting set of five photometric bands is much better able to disentangle multiple stellar populations, which are also distinguished on the basis of their CNO content. We are also computing a new stellar-evolution library, including varying chemical compositions, which will enable us to interpret our new photometry in terms of MPs in GCs. In particular the new models include variation of CNO content, which has a strong impact on age estimates (Cassisi et al. 2008; Ventura et al. 2009). The final product will be a new estimate of relative ages for the different populations, This will be done with a precision that has never been attained before.

8.16. Binaries in Multiple Stellar Populations

An accurate study of the CMD can provide information on the population of binary systems in GCs, such as the fraction of MS–MS binaries, the distribution of mass ratios, and the radial distribution (see, e.g., Romani & Weinberg 1991; Sollima et al. 2007; Milone et al. 2012c). These are fundamental ingredients for understanding the dynamical evolution of GCs and their population of exotic stellar objects, such as BSSs, cataclysmic variables, millisecond pulsars, and low-mass X-ray binaries. We plan to exploit the large number of CMDs that can be obtained from our data set to refine our previous investigations on binary fraction, binary mass distribution, and binary radial distribution (Milone et al. 2012c), which was based on F606W and F814W photometry only. Moreover, in clusters with multiple MSs, we will estimate the fraction of binaries in the different stellar populations.

8.17. Blue Straggler Stars

BSSs are crucial probes of the internal dynamics of GCs (e.g., Ferraro et al. 2012). Since they are hotter than 6000–7000 K, they are best detectable at UV wavelengths, so we can use the UV survey data to obtain complete samples of BSSs in the central regions of GCs with a significant improvement in completeness over that of previous efforts (e.g., Piotto et al. 2004). Detailed star counts and complete luminosity functions will be obtained, possible sub-structure unveiled (such as the double sequences in M30 and NGC 362; Ferraro et al. 2009b; Dalessandro et al. 2013b), and extended

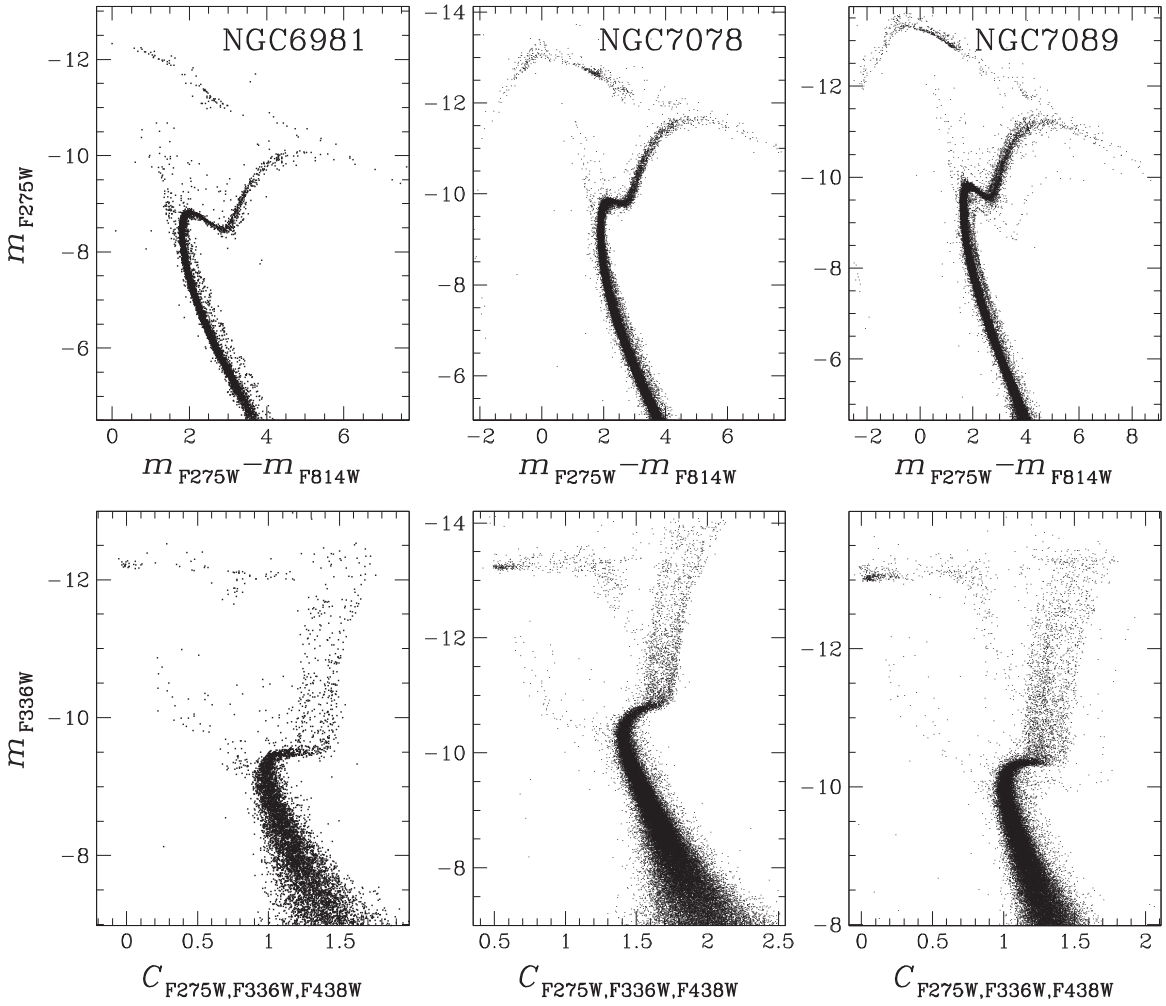

Figure 22. As in Figure 4, for NGC 6981, NGC 7078, and NGC 7089.

radial distributions will be derived from combination with wider-field ground-based observations.

8.18. Stellar Exotica

The UV survey will be used to search for exotic objects that came from the evolution of binary systems in the cores of GCs. Among these, of particular interest is the identification of the companion stars in binary millisecond pulsars (Ferraro et al. 2001, 2003b; Pallanca et al. 2010), since it would allow us to quantify the occurrence of dynamical interactions and to constrain the mass of neutron stars, with invaluable consequences for the equation of state of matter at equilibrium densities that are near nuclear.

8.19. Cross Correlation of X-ray Sources with HST UV/Optical Data

More generally, studies of the nature, origin, and evolution of binary stars and their progeny will be aided by cross-correlation of the GO-13297 data with imaging at X-ray wavelengths. As repositories of energy, binaries play a central role in the dynamics of GCs. With sub-arcsecond positions provided by the *Chandra X-ray Observatory*, whose archive already includes more than half of the survey clusters, optical and/or UV counterparts can be identified for a wide variety of systems. These include cataclysmic variables, quiescent low-mass X-ray binaries, millisecond pulsars, red stragglers, and systems with active coronae (e.g., RS, CVn, and BY Dra stars). PMs measured as a part of this program will make the additional contribution of separating binaries and stellar exotica from field stars that occupy the same regions of the CMD.

8.20. Luminosity and Mass Functions of Different Stellar Populations

GO-10775 allowed us to extract the stellar mass functions for 17 GCs (Paust et al. 2010). With the new data we plan to extend this survey; this will have important implications, in particular for the effect of the Galactic gravitational potential (Djorgovski et al. 1993) on the GC stellar mass function. Moreover, from CMDs that now include UV colors, with which multiple MSs are better distinguished, we should be able to obtain the mass functions of the different stellar populations in the same cluster, as Milone et al. (2012d) did for NGC 2808.

8.21. Galactic Bulge Globular Clusters

Multi-populations have been detected in a few massive Galactic-bulge GCs, but so far no systematic search for them has been undertaken. About half a dozen clusters in the GO-13297 target list are located in the inner bulge or at the edge of

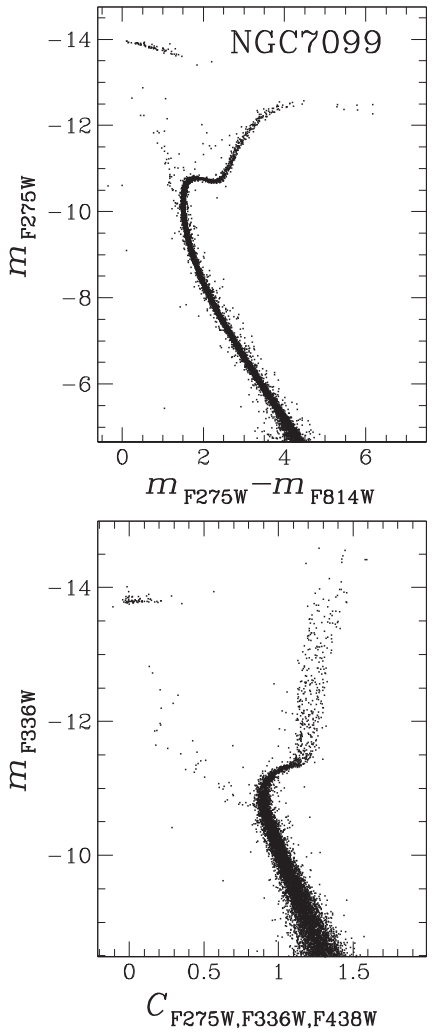

Figure 23. As in Figure 4, for NGC 7099.

the bulge/halo transition zone, and may be dynamically connected to the bulge. The bulge clusters have different properties from the classical halo clusters, and there is evidence that they formed in an early epoch (Barbuy et al. 1998; Coté 1999). The metal-rich clusters there might show a high helium abundance.

A few other clusters show a blue HB and a metallicity $[\mathrm{Fe/H}] \geqslant -1.0$. Therefore these GCs are either very old or else they host at least two stellar populations.

8.22. Spectral Energy Distributions of Multiple Stellar Populations

We will use the multi-band photometry to calculate integrated cluster UV/optical colors by summing the flux of all measured stars in order to obtain an integrated-color database that can be used for the study of extragalactic GCs. More generally, GCs are widely used as template stellar populations for the calibration of stellar evolutionary sequences and of the synthetic stellar populations that are constructed with them. These are then used to interpret the light from very distant galaxies, including the rest-frame UV. The multiband database resulting from this Treasury program will constitute the main benchmark for this indispensable calibration.

8.23. Link between Globular Cluster UV Properties and Extragalactic Sources

With these data it will be possible to calibrate integrated cluster UV/optical colors for the diagnostics of MPs in unresolved stellar systems, such as GCs in galaxies well beyond the Local Group, exploring to what extent the formation of GCs has proceeded in a similar (or different) fashion in different galactic environments, e.g., in ellipticals versus spirals. Indeed, the suspicion exists that several massive GCs in the giant elliptical M87 may harbor helium-enriched populations as revealed by UV excess, likely due to the presence of very hot 2G HB stars (e.g., Kaviraj et al. 2007).

8.24. Differential Reddening Analysis and Reddening Maps

The interstellar medium exhibits complex structure, on scales ranging from a few astronomical units to several kiloparsecs (e.g., Schlegel et al. 1998). We plan to determine for each cluster a high-resolution map (typically around 10 square arcsec) of differential reddening (as in Milone et al. 2012b, Section 3). Correcting photometry for differential reddening is a crucial step for identifying multiple stellar populations in the CMD of any GC.

8.25. UV Photometric Standards

To date there is no large space-based network of UV photometric standards. We propose to use *HST* UV archival material to improve the existing absolute photometric calibration of WFC3/UVIS in F275W and F336W bands, and to build a network of photometric standards that will remain a fundamental reference for years to come. GO-13297 GCs are rather evenly distributed in the sky and contain hundreds of bright and relatively isolated (at least in UV images) stars that can be used to calibrate other UV instruments and the ground-based *U*-band observations. This is particularly valuable taking into account that after *HST*, no other large space-based observatory with UV capability is expected to fly for at least 10 years.

8.26. Serendipity

We are certain that in addition to those mentioned above, this multi-band legacy database for Galactic GCs will offer unlimited possibilities for serendipitous discoveries and an extremely wide variety of other scientific investigations, and will contribute to our understanding of the formation of our Galaxy itself.

A.A., S.C., S.H., M.M., and G.P. recognize partial support by the IAC (grant P301031) and the Ministry of Competitiveness and Innovation of Spain (grant AYA2010-16717). J.A., A.C., I.R.K., A.S., and E.V. acknowledge support from STScI grant GO-13297. A.P.M. acknowledges support by the Australian Research Council through Discovery Project grant DP120100475. M.Z. acknowledges support by Proyecto Fondecyt Regular 1110393, by the BASAL Center for Astrophysics and Associated Technologies PFB-06, and by Project IC120009 "Millennium Institute of Astrophysics (MAS)" of Iniciativa Científica Milenio by the Chilean Ministry of Economy, Development and Tourism. F.R.F., B.L. and E.D. acknowledge the support from the Cosmic-Lab project (web site: http://www.cosmic-lab.eu) funded by the

European Research Council, under contract ERC-2010-AdG-267675.

REFERENCES

Anderson, J., Sarajedini, A., Bedin, L. R., et al. 2008, AJ, 135, 2055
Anderson, J., & Bedin, L. R. 2010, PASP, 122, 1035
Anderson, J., & van der Marel, R. P. 2010, ApJ, 710, 1032
Bastian, N., Cabrera-Ziri, I., Davies, B., & Larsen, S. S. 2013a, MNRAS, 436, 2852
Bastian, N., Lamers, H. J. G. L. M., de Mink, S. E., Longmore, S. N., Goodwin, S. P., & Gieles, M. 2013b, MNRAS, 436, 2398
Barbuy, B., Bica, E., & Ortolani, S. 1998, A&A, 333, 117
Bedin, L. R., Piotto, G., Anderson, J., et al. 2004, ApJ, 605, L125
Bedin, L. R., King, I. R., Anderson, J., et al. 2008, ApJ, 678, 1279
Bekki, K. 2011, MNRAS, 412, 2241
Bellini, A., Piotto, G., Bedin, L. R., et al. 2009, A&A, 507, 1393
Bellini, A., Bedin, L. R., Piotto, G., et al. 2010, AJ, 140, 631
Bellini, A., Piotto, G., Milone, A. P., et al. 2013a, ApJ, 765, 32
Bellini, A., van der Marel, R. P., & Anderson, J. 2013b, MmSAI, 84, 140
Bellini, A., Anderson, J., van der Marel, R. P., et al. 2014, ApJ, submitted
Brown, T. M., Sweigart, A. V., Lanz, T., Landsman, W. B., & Hubeny, I. 2001, ApJ, 562, 368
Brown, T. M., Sweigart, A. V., Lanz, T., et al. 2010, ApJ, 718, 1332
Busso, G., Cassisi, S., Piotto, G., et al. 2007, A&A, 474, 105
Caloi, V., & D'Antona, F. 2007, A&A, 463, 949
Campbell, S. W., Yong, D., Wylie-de Boer, E. C., et al. 2010, MmSAI, 81, 1004
Campbell, S. W., D'Orazi, V., Yong, D., et al. 2013, Natur, 498, 198
Carretta, E., Bragaglia, A., Gratton, R. G., et al. 2009, A&A, 505, 117
Carretta, E., Bragaglia, A., Gratton, R. G., et al. 2010, A&A, 520, A95
Cassisi, S., Salaris, M., Pietrinferni, A., et al. 2008, ApJL, 672, L115
Cassisi, S., Marín-Franch, A., Salaris, M., et al. 2011, A&A, 527, A59
Cassisi, S., Mucciarelli, A., Pietrinferni, A., Salaris, M., & Ferguson, J. 2013, A&A, 554, A19
Cassisi, S., & Salaris, M. 2014, A&A, 563, A10
Coté, P. 1999, AJ, 118, 406
Da Costa, G. S., Held, E. V., & Saviane, I. 2014, MNRAS, 438, 3507
Dalessandro, E., Salaris, M., Ferraro, F. R., et al. 2011, MNRAS, 410, 694
Dalessandro, E., Salaris, M., Ferraro, F. R., Mucciarelli, A., & Cassisi, S. 2013, MNRAS, 430, 459
Dalessandro, E., Ferraro, F. R., Massari, D., et al. 2013, ApJ, 778, 135
D'Antona, F., Gratton, R., & Chieffi, A. 1983, MmSAI, 54, 173
D'Antona, F., Caloi, V., Montalbán, J., Ventura, P., & Gratton, R. 2002, A&A, 395, 69
D'Antona, F., & Caloi, V. 2004, ApJ, 611, 871
D'Antona, F., & Caloi, V. 2008, MNRAS, 390, 693
D'Antona, F., Ventura, P., Decressin, T., Vesperini, E., & D'Ercole, A. 2014, MNRAS, 443, 3302
D'Cruz, N. L., Dorman, B., Rood, R. T., & O'Connell, R. W. 1996, ApJ, 466, 359
Decressin, T., Meynet, G., Charbonnel, C., Prantzos, N., & Ekström, S. 2007, A&A, 464, 1029
Decressin, T., Baumgardt, H., Charbonnel, C., & Kroupa, P. 2010, A&A, 516, A73
de Mink, S. E., Pols, O. R., Langer, N., & Izzard, R. G. 2009, A&A, 507, L1
D'Ercole, A., Vesperini, E., D'Antona, F., McMillan, S. L. W., & Recchi, S. 2008, MNRAS, 391, 825
D'Ercole, A., D'Antona, F., & Vesperini, E. 2011, MNRAS, 415, 1304
Djorgovski, S., Piotto, G., & Capaccioli, M. 1993, AJ, 105, 2148
Ferraro, F. R., Possenti, A., D'Amico, N., & Sabbi, E. 2001, ApJ, 561, L93
Ferraro, F. R., Possenti, A., Lagani, P., et al. 2003a, in ASP Conf. Proc. 296, New Horizons in Globular Cluster Astronomy, ed. G. Piotto, et al. (San Francisco, CA: ASP), 143
Ferraro, F. R., Possenti, A., Sabbi, E., & D'Amico, N. 2003b, ApJL, 596, L211
Ferraro, F. R., Dalessandro, E., Mucciarelli, A., et al. 2009a, Natur, 462, 483
Ferraro, F. R., Beccari, G., Dalessandro, E., et al. 2009b, Natur, 462, 1028
Ferraro, F. R., Lanzoni, B., Dalessandro, E., et al. 2012, Natur, 492, 393
Geisler, D., Villanova, S., Carraro, G., et al. 2012, ApJL, 756, L40
Gratton, R. G., Lucatello, S., Carretta, E., et al. 2011, A&A, 534, A123
Gratton, R. G., Lucatello, S., Carretta, E., et al. 2012, A&A, 539, A19
Gratton, R. G., Lucatello, S., Sollima, A., et al. 2013, A&A, 549, A41
Harris, W. E. 1996, AJ, 112, 1487
Kaviraj, S., Schawinski, K., Devriendt, J. E. G., et al. 2007, ApJS, 173, 619
King, I. R., Bedin, L. R., Piotto, G., Cassisi, S., & Anderson, J. 2005, AJ, 130, 626
King, I. R., Bedin, L. R., Cassisi, S., et al. 2012, AJ, 144, 5
Lanzoni, B., Mucciarelli, A., Origlia, L., et al. 2013, ApJ, 769, 107
Lardo, C., Bellazzini, M., Pancino, E., et al. 2011, A&A, 525, A114
Lützgendorf, N., Kissler-Patig, M., Gebhardt, K., et al. 2013, A&A, 552, A49
MacKenty, J. W., & Smith, L. J. 2012, CTE White Paper, http://www.stsci.edu/hst/wfc3/ins_performance/CTE/CTE_White_Paper.pdf
Marín-Franch, A., Aparicio, A., Piotto, G., et al. 2009, ApJ, 694, 1498
Marino, A. F., Milone, A. P., & Lind, K. 2013, ApJ, 768, 27
Marino, A. F., Milone, A. P., Piotto, G., et al. 2009, A&A, 505, 1099
Marino, A. F., Milone, A. P., Piotto, G., et al. 2011b, ApJ, 731, 64
Marino, A. F., Milone, A. P., Piotto, G., et al. 2012, ApJ, 746, 14
Marino, A. F., Milone, A. P., Przybilla, N., et al. 2014, MNRAS, 437, 1609
Marino, A. F., Sneden, C., Kraft, R. P., et al. 2011c, A&A, 532, A8
Marino, A. F., Villanova, S., Piotto, G., et al. 2008, A&A, 490, 625
Marino, A. F., Villanova, S., Milone, A. P., et al. 2011a, ApJL, 730, L16
Milone, A. P., Marino, A. F., Bedin, L. R., et al. 2014, MNRAS, 439, 1588
Milone, A. P., Marino, A. F., Dotter, A., et al. 2014, ApJ, 785, 21
Milone, A. P., Marino, A. F., Piotto, G., et al. 2012, ApJ, 745, 27
Milone, A. P., Marino, A. F., Piotto, G., et al. 2013, ApJ, 767, 120
Milone, A. P., Marino, A. F., Piotto, G., et al. 2015, MNRAS, 447, 931
Milone, A. P., Piotto, G., Bedin, L. R., et al. 2012, ApJ, 744, 58
Milone, A. P., Piotto, G., Bedin, L. R., et al. 2012, A&A, 540, A16
Milone, A. P., Piotto, G., Bedin, L. R., et al. 2012, A&A, 537, A77
Milone, A. P., Piotto, G., King, I. R., et al. 2010, ApJ, 709, 1183
Miocchi, P., Lanzoni, B., Ferraro, F. R., et al. 2013, ApJ, 774, 151
Norris, J., Cottrell, P. L., Freeman, K. C., & Da Costa, G. S. 1981, ApJ, 244, 205
Norris, J. E., & Da Costa, G. S. 1995, ApJ, 447, 680
Norris, J. E. 2004, ApJL, 612, L25
Noyola, E., Gebhardt, K., Kissler-Patig, M., et al. 2010, ApJL, 719, L60
Pallanca, C., Dalessandro, E., Ferraro, F. R., et al. 2010, ApJ, 725, 1165
Paust, N. E. Q., Reid, I. N., Piotto, G., et al. 2010, AJ, 139, 476
Pilachowski, C., Sneden, C., Kraft, R. P., & Langer, G. E. 1996, BAAS, 28, 821
Piotto, G., de Angeli, F., King, I. R., et al. 2004, ApJL, 604, L109
Piotto, G., Villanova, S., Bedin, L. R., et al. 2005, ApJ, 621, 777
Piotto, G., Bedin, L. R., Anderson, J., et al. 2007, ApJL, 661, L53
Piotto, G., Milone, A. P., Anderson, J., et al. 2012, ApJ, 760, 39
Piotto, G., Milone, A. P., Marino, A. F., et al. 2013, ApJ, 775, 15
Renzini, A. 2008, MNRAS, 391, 354
Renzini, A. 2013, MmSAI, 84, 162
Rich, R. M., Sosin, C., Djorgovski, S. G., et al. 1997, ApJL, 484, L25
Richer, H. B., Heyl, J., Anderson, J., et al. 2013, ApJL, 771, L15
Romani, R. W., & Weinberg, M. D. 1991, in ASP Conf. Proc. 13, The Formation and Evolution of Star Clusters, ed. K. Janes (San Francisco, CA: ASP), 443
Rood, R. T., & Crocker, D. A. 1989, in IAU Coll. 111, The Use of Pulsating Stars in Fundamental Problems of Astronomy , ed. E. G. Schmidt (Cambridge: Cambridge Univ. Press), 103
Salaris, M., & Cassisi, S. 2014, A&A, 566, A109
Schaerer, D., & Charbonnel, C. 2011, MNRAS, 413, 2297
Sbordone, L., Salaris, M., Weiss, A., & Cassisi, S. 2011, A&A, 534, A9
Schlegel, D. J., Finkbeiner, D. P., & Davis, M. 1998, ApJ, 500, 525
Sollima, A., Ferraro, F. R., Bellazzini, M., et al. 2007, ApJ, 654, 915
Trenti, M., & van der Marel, R. 2013, MNRAS, 435, 3272
Vanbeveren, D., Mennekens, N., & De Greve, J. P. 2012, A&A, 543, A4
van der Marel, R. P., & Anderson, J. 2010, ApJ, 710, 1063
Ventura, P., Caloi, V., D'Antona, F., et al. 2009, MNRAS, 399, 934
Ventura, P., Criscienzo, M. D., D'Antona, F., et al. 2014, MNRAS, 437, 3274
Vesperini, E., McMillan, S. L. W., D'Antona, F., & D'Ercole, A. 2010, ApJL, 718, L112
Vesperini, E., McMillan, S. L. W., D'Antona, F., & D'Ercole, A. 2013, MNRAS, 429, 1913
Villanova, S., Geisler, D., Piotto, G., & Gratton, R. G. 2012, ApJ, 748, 62
Villanova, S., Geisler, D., Carraro, G., Moni Bidin, C., & Muoz, C. 2013, ApJ, 778, 186
Vinkó, J., Sárneczky, K., Balog, Z., et al. 2009, ApJ, 695, 619
Walker, A. R., Kunder, A. M., Andreuzzi, G., di Cecco, A., & Stetson, P. B. 2011, MNRAS, 415, 643
Yong, D., & Grundahl, F. 2008, ApJL, 672, L29
Yong, D., Grundhal, F., Johnson, J. A., & Asplund, M. 2008, ApJ, 684, 1159
Yong, D., Roederer, I. U., Grundahl, F., et al. 2014, MNRAS, 441, 3396